Chemical biology studies on retaining exo-β-glucosidases

Su, Q.

Chapter 3

Selective labelling of GBA2 in cells with fluorescent β-D-arabinofuranosyl cyclitol aziridines

Taken in part from:

Qin Su, Max Louwerse, Rob F. Lammers, Elmer Maurits, Max Janssen, Rolf G. Boot, Valentina Borlandelli, Wendy A. Offen, Daniël Linzel, Sybrin P. Schröder, Gideon J. Davies, Herman S. Overkleeft, Marta Artola, Johannes M. F. G. Aerts. *Chem. Sci.* doi.org/10.1039/D3SC06146A.

Abstract

GBA2, the non-lysosomal β-glucosylceramidase, is an enzyme involved in glucosylceramide metabolism. Pharmacological inhibition of GBA2 by *N*-alkyl iminosugars is well tolerated and benefits patients suffering from Sandhoff and Niemann-Pick type C diseases, and GBA2 inhibitors have been proposed as candidate-clinical drugs for the treatment of Parkinsonism. With the ultimate goal to unravel the role of GBA2 in (patho)physiology, this chapter describes the development of a GBA2-selective activity-based probe (ABP). A library of probes was tested for activity against GBA2 and the two other cellular retaining β-glucosidases, lysosomal GBA1 and cytosolic GBA3. It is shown that β-D-arabinofuranosyl cyclitol aziridine (β-D-Ara*f* aziridine) reacts with the GBA2 active site nucleophile to form a covalent and irreversible bond. Fluorescent β-D-Ara*f* aziridine probes potently and selectively label GBA2 both *in vitro* and *in situ*, allowing for visualization of subcellular localization of overexpressed GBA2 using fluorescence microscopy. The here-presented ABP technology may be useful for further delineating the role and functioning of GBA2 in disease. As well, the β-D-Ara*f* aziridine scaffold may serve as a good starting point for the development of GBA2-specific inhibitors for clinical development.

Introduction

GBA2 (EC 3.2.1.45, CAZy[1] GH116), a retaining β-glucosidase, was first discovered during the analysis of N-[6-[(7-nitro-2-1,3-benzoxadiazol-4-yl)amino]hexanoyl]-β-D-glucosylceramide (NBD-GlcCer) processing in cultured cells. Ensuing studies demonstrated that GBA2, initially named non-lysosomal glucosylceramidase, is capable of hydrolyzing glucosylceramide (GlcCer), which until that date was thought to be the exclusive activity of the enzyme deficient in Gaucher disease (GD), lysosomal glucocerebrosidase (GBA1, EC 3.2.1.45, GH30).[2] GBA2 is now implicated in several inherited metabolic disorders.[3-6] As well, companies have announced the development of GBA2 inhibitors for the treatment of Parkinsonism.[7] Despite this, the physiological role of GBA2, the consequences of cytosolic GlcCer metabolism and the interplay of GBA2 with lysosomal GlcCer breakdown is unclear.

GBA2 is a tightly membrane-bound enzyme whose activity can be assessed in cell and tissue lysates using the artificial fluorogenic substrate, 4-methylumbelliferyl-β-D-glucopyranoside (4MU-β-D-Glc). Compared to GBA1, GBA2 is less sensitive to inactivation by conduritol B epoxide (CBE), but more susceptible to inactivation by various detergents.[2] The loss of enzymatic activity following its extraction from membranes complicates its purification, and the enzyme's identity was definitively elucidated only after the independent cloning of its cDNA.[8,9] GBA2 homologues are found in several species, including archaea and bacteria,[10,11] and GBA2 proteins degrading glucosylceramide are found, besides mammals, in plant and fish.[12-15] To date mammalian GBA2 has defied resolution of a 3D structure, but structures of bacterial homologs (such as SSO1353 (GH116) in *S. solfataricus* and *Tx*GH116 in *T. xylanolyticum*[10,11,16]) provide insight in the catalytic machinery of the enzyme.

Human GBA2 is encoded by the *GBA2* gene at locus *9p13.3* and is a 927 amino acid β-glucosidase with E527 as the catalytic nucleophile and D677 as the catalytic acid/base.[17] It is a retaining glycosidase processing its substrate following a classical Koshland double displacement mechanism. GBA2 is initially synthesized as a soluble cytosolic protein that rapidly and tightly associates with membranes by an unknown mechanism. Various subcellular localizations of (overexpressed, tagged) GBA2 have been reported, ranging from endoplasmic reticulum, Golgi apparatus, endosomes and the plasma membrane.[9,18] The enzyme's localization possibly varies among cells, perhaps reflecting their metabolic status. Unlike GBA1, GBA2 is able to hydrolyze both β-glucoside and β-galactoside substrates.[2] GBA2 can also act as a transglycosidase, transferring glucose from GlcCer to, for instance, cholesterol, further adding to the mystery of the physiological role of GBA2.[19,20]

GBA2 is increasingly considered as therapeutic target for the treatment of a variety of diseases. Inhibition of GBA2 is a side effect of *N*-butyl-deoxynojirimycin (Miglustat), a registered treatment for GBA1-deficient type 1 GD and Niemann Pick disease type C (NPC) patients. Miglustat acts by pharmacological inhibition of glucosylceramide synthase (GCS).[21-23] Individuals under this treatment appear to develop no overt side effects upon long-term therapy. In line with this, inhibition of GBA2 activity with *N*-adamantanemethyloxypentyl-deoxynojirimycin (AMP-DMN) or its genetic ablation has been found to increase the life span of NPC mice.[22] Tissues of NPC mice show partial increase in GBA2 and partial reduced GBA1 levels suggesting a compensatory mechanism between these enzymes.[15] In type 1 GD mice generated by knockdown of GBA1 in a hematopoietic stem cell lineage, GBA2 gene deletion was found to exert beneficial effects.[24] In addition, increased GBA2 activities have been documented in leukocytes of GBA1-deficient GD patients.[25] Finally and importantly, GBA2 knockout (KO) mice develop no overt pathology besides partially reduced fertility, a phenomenon not observed in primates.[10,26]

Several classes of GBA2 inhibitors have been identified in the past decades. Competitive GBA2 inhibitors include iminosugars such as AMP-DNM, with an IC_{50} of approximately 1 nM with respect to GBA2, and *N*-butyl-deoxynojirimycin (Miglustat), with an IC_{50} of 150-300 nM for GBA2.[27] Mechanism-based, covalent and irreversible inhibitors, such as cyclophellitol aziridine act on GBA2 but also on GBA1, and activity-based probes (ABPs) derived from these cannot be used for selective GBA2 detection and imaging in cells.[28]

For this reason the aim was to develop a GBA2-selective activity-based probe for *in cellulo* GBA2 imaging, and the results of studies in this direction are presented here.[29] Previous studies showed the

value of cyclophellitols as GBA1-specific probes,[15,30] however the closely related cyclophellitol aziridine ABPs (ABP **7** and **8**, Figure 1) label both GBA1 and GBA2.[28,31] Some cell types also express a soluble, cytosolic β-glucosidase with broad substrate specificity, termed GBA3 (EC 3.2.1.21, GH1), which also reacts with these ABPs.[28] Since none of these ABPs react selectively with GBA2, cyclophellitol-type compounds with varying configurations were investigated on their reactivity with GBA2 and related cellular retaining β-glucosidases. The findings of these studies, detailed in this chapter, demonstrate that ABPs with a β-D-Ara*f* aziridine configuration (Figure 1) potently and selectively label GBA2 by reacting with its catalytic nucleophile.

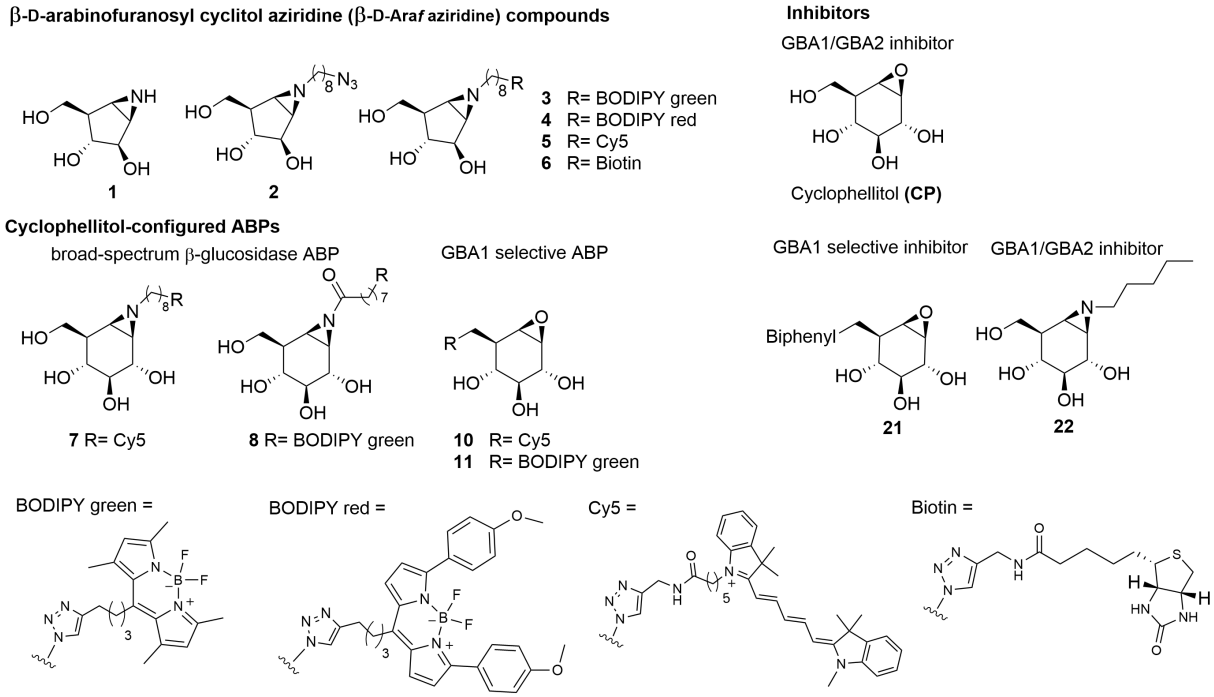

Figure 1. Chemical structures of β-D-arabinofuranosyl cyclitol aziridine **1**-**6**, cyclophellitol epoxide and aziridine activity-based probes (ABPs) **7**-**11**, and inhibitors **21** and **22**.

Results

In vitro affinity and selectivity of β-D-Ara*f* cyclitol aziridine ABPs towards human β-glucosidases

To identify an ABP that selectively labels human GBA2 over GBA1 and GBA3, a library of cyclophellitol-based ABPs with varying configurations (Figure S1) was screened for their selectivity towards human retaining β-glucosidases. For this purpose, the inhibition properties of the compounds were first assessed using recombinant human GBA1 (rhGBA1, Imiglucerase), lysates of cells overexpressing GBA2 and lysates overexpressing GBA3, the latter two both in combination with knockout of the other retaining β-glucosidases. In a preliminary screen, enzymes were pre-incubated for 30 min with the tested compounds, followed by the addition of the fluorogenic substrate, 4MU-β-D-Glc, and then quantification of released fluorescent 4MU after 30 minutes. This screening revealed a set of β-D-Ara*f* cyclitol aziridines as potential GBA2 inhibitors. Pre-incubation of the enzymes with β-D-Ara*f* cyclitol aziridine **1** did not show inhibitory effect towards any of the β-glucosidases assayed up to 50 µM, whereas *N*-azido-octyl aziridine **2** displayed inhibition of all three β-glucosidases (apparent IC_{50}: GBA2 630 nM, GBA1 2730 nM, GBA3 8150 nM) with some selectivity for GBA2 over GBA1 and GBA3 (Table S1). Interestingly, BODIPY green- and BODIPY red-tagged ABPs **3** and **4** exhibited substantial affinity towards GBA2 (apparent IC_{50}: 120-160 nM) with clear selectivity (defined as IC_{50} Enzyme1/IC_{50} Enzyme2) for GBA2 over GBA1 and GBA3 (Figure 2A). In contrast, β-D-Araf ABP **5** equipped with a Cy5 fluorophore inhibited GBA1 and GBA2 with about equal potency (apparent IC_{50} 250-300 nM). The biotin-tagged β-D-Ara*f* compound **6** is a poor (apparent IC_{50} > 8 µM) inhibitor of all three glucosidases.

Arabinofuranosyl cyclitol **12**-**20** with various configurations (α-L-Ara*f* and β-L-Ara*f*) were also evaluated (Figure S1). Most of these proved to be poor GBA2 inhibitors (apparent IC_{50} > 20 μM), and none matched the selectivity of β-D-Ara*f* cyclitol aziridines **3** and **4** for GBA2 (Table S1).

Armed with ABPs **3** and **4**, both of which displayed high selectivity for GBA2 over GBA1 and GBA3, their activity in cell lysates was analyzed next. To this end, lysates of HEK293T cells containing all three β-glucosidases (endogenous GBA1 with overexpressed GBA2 and GBA3) were treated with ABPs **3**, **4**, **5** and **7**, followed by protein separation by SDS-PAGE and fluorescence scanning of the wet gel slabs. As depicted in Figure 2B, ABP **7** labelled all β-glucosidases as previously reported.[31] In contrast, the β-D-Ara*f* aziridine ABPs **3** and **4** selectively labelled GBA2 at a concentration of 100 nM, while Cy5 tagged ABP **5** did so at 500 nM. The GBA2 selectivity of β-D-Ara*f* cyclitol aziridines **3**, **4** and **5** was confirmed in a mixture of a lysate of cells overexpressing GBA2 with rhGBA1 (Figure 2C and Figure S3). In this experiment, the enzyme mixture was first incubated with β-D-Ara*f* aziridine ABPs **3**, **4**, or **5** for 30 minutes, after which selective GBA1 ABP **10**[32] or **11**[30] was added to label the remaining active rhGBA1 molecules. This experiment revealed the ability of β-D-Ara*f* cyclitol aziridine ABPs, and in particular **3** and **4**, to selectively label GBA2 without significant rhGBA1 labelling, with marginal GBA1 labelling occurring at 10 μM.

The pH and incubation time dependent labelling of GBA2 in HEK293T cells containing all three retaining β-glucosidases by β-D-Ara*f* ABPs was next investigated (Figure 2D, E and Figure S4). All ABPs selectively label GBA2 at a pH range of 4.5-7.5. Using 500 nM of ABP **4**, GBA2 labelling occurred within a minute, and maximal labelling was observed after 20-30 minutes. Importantly, no labelling of GBA1 or GBA3 was observed under varying pH and time conditions (Figure S4).

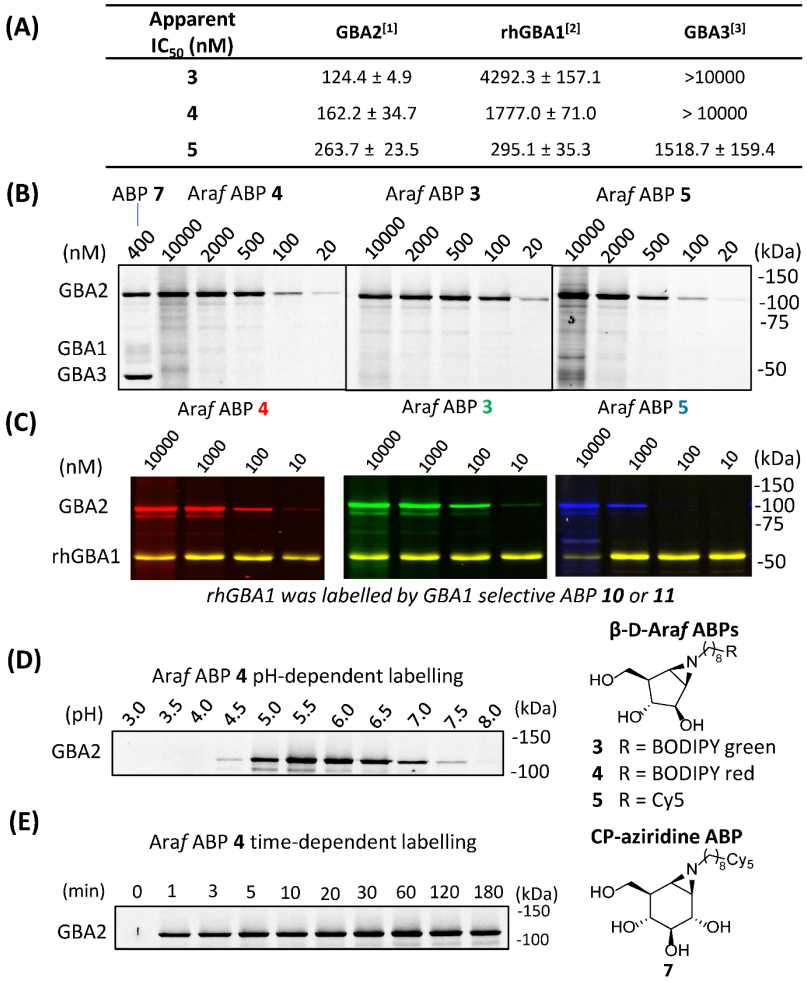

Figure 2. *In vitro* ABPP with β-D-Ara*f* aziridine ABPs **3**-**5**. (A) Apparent IC_{50} (nM) of β-D-Ara*f* ABPs, determined by 4MU-β-D-Glc fluorogenic substrate assay, enzyme: [1] GBA2 = GBA1/GBA2 KO HEK293T cell lysates with GBA2 overexpression (OE), [2] rhGBA1 = isolated recombinant Imiglucerase (Cerezyme®). [3] GBA3 = GBA1/GBA2 KO HEK293T cell lysates with GBA3 OE. Error ranges = ± SD, n = 3 replicates. (B) HEK293T cell lysates expressing endogenous GBA1 and overexpressed GBA2/GBA3 were used as enzyme source. Lysates were treated with ABPs **3**-**5** for 30 min at pH 6.0. (C) Mixture of GBA1/GBA2 KO HEK293T with GBA2 OE lysate and rhGBA1 were incubated with β-D-Ara*f* ABPs (**3**-**5**) for 30 min at pH 5.8, following addition of 500 nM of ABP **10** (for **3** and **4**) or ABP **11** (for **5**). (D) *In vitro* pH-dependent labelling of ABP **4** (500 nM). (E) *In vitro* time-dependent ABPP assay of ABP **4** (500 nM).

Identification of the catalytic nucleophile of GBA2 reacted with β-D-Ara*f* cyclitol aziridines

GBA2, like *Tx*GH116 (the bacterial homologue of GBA2), induces hydrolysis through a conventional Koshland two-step double-displacement conformational pathway typical of retaining β-glucosidases, progressing from $^{1}S_{3}$ to $^{4}H_{3}$ to ultimately adopt the $^{4}C_{1}$ in the covalent complex (Figure 3A).[11] In contrast to cyclophellitol aziridines, which mimic the $^{4}H_{3}$ transition state, β-D-Ara*f* aziridines adopt an ^{3}E conformation[33] which resembles the $^{1}S_{3}$ initial Michaelis complex conformation (Figure 3B).[34] Previous research had established that E527 (catalytic nucleophile) and D677 (catalytic acid/base) are the catalytic residues in the human GBA2 active site.[17] To investigate whether β-D-Ara*f* aziridine ABPs bind GBA2 in an activity-based manner, firstly mutants of GBA2 were generated by substituting either the E527 nucleophile or the D677 acid/base. Lysates from cells expressing these mutant GBA2 proteins were then incubated with β-D-Ara*f* ABPs **3**-**5** or cyclophellitol ABP **7** and their labelling pattern was analyzed (Figure 3C). None of the ABPs were found to label the E527G mutant or the E527G/D677G double mutant, demonstrating that these probes require the nucleophile E527 for reaction with GBA2. Notably, β-D-Ara*f* ABPs **3**-**5** exhibit poor reaction with the acid/base mutant D677G, whereas ABP **7**

modified this mutant in significant amounts. At higher ABP concentrations and/or longer incubation times (Figure 3D) some degree of labelling of the acid/base mutant GBA2 was detected also with ABPs **3**-**5**.

To firmly establish the mode of action of β-D-Ara*f* cyclitol aziridines as mechanism-based GBA2 inhibitors, the 3D structure of the GH116 bacterial GBA2 homolog, *Tx*GH116 from *Thermoanaerobacterium xylanolyticum* in complex with β-D-Ara*f* compound **2** was solved at 1.9 Å resolution. The -1 subsite of TxGH116 is well conserved relative to human GBA2. The solved structure (Figure 3E) reveals reacted **2** with the catalytic nucleophile of *Tx*GH116, occupying the enzyme active site anchored by several hydrogen bonds. The OH group on C2 interacts with NE2 His507 and OD2 Asp452, and the OH on C3 with OD2 Asp452, NH2 Arg792 and OG1 and the alcohol of Thr591. The OH on C5 is hydrogen-bonded to OE2 Glu777 and to NH1 and NH2 Arg786. In addition, the amine from the ring-opened aziridine group forms a hydrogen bond to OD2 Asp593 and to a water molecule (which also interacts with OD1 Asp593). There is insufficient electron density to allow modelling of the end of the azidooctyl group, which extend into a more open region at the edge of the protein where they are less constrained.

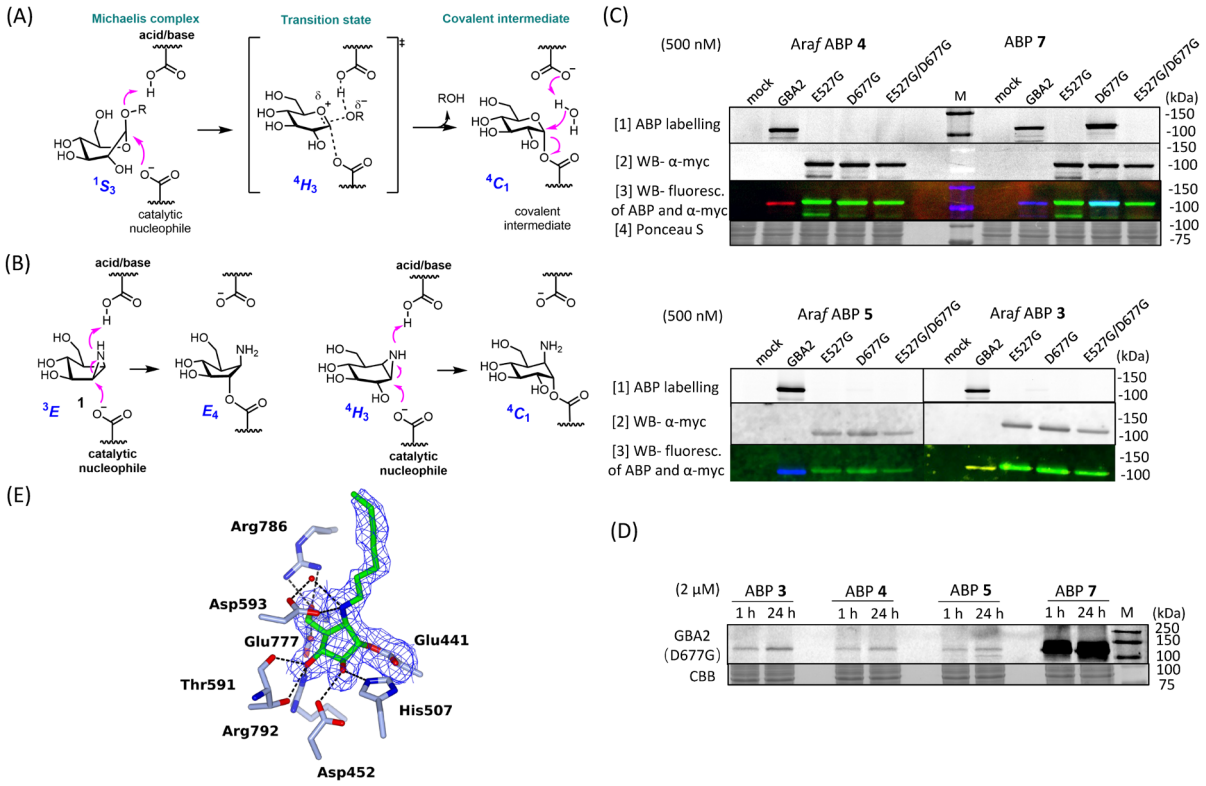

Figure 3. Mechanism of inhibition of GBA2 by β-D-Ara*f* cyclophellitol aziridines. (A) Conformational itinerary of the Koshland double-displacement mechanism employed by retaining β-D-glucosidases. (B) β-D-Ara*f* cyclitol aziridine **1** adopts an envelope-like ^{3}E conformation prior to reaction with the GBA2 active site, whereas cyclophellitol aziridines mimic the $^{4}H_{3}$ transition state conformation. (C) β-D-Ara*f* aziridine ABPs (**3**-**5**) and cyclophellitol aziridine ABP **7** labelling of lysates of HEK293T cells overexpressing myc-tagged mutant (E527G, D677G or E527G/D677G) or wildtype GBA2. mock = HEK293T GBA1/GBA2 KO cell lysate, GBA2 = HEK293T GBA1/GBA2 KO GBA2 OE cell lysate. Gel images were captured by fluorescence scanning on wet gel slabs (row 1) and Western blot (nitrocellulose membrane) using an anti-myc antibody (row 2). Row 3 represents the Western blot showing fluorescence of both ABPs (**3**-**5**, **7**) and the anti-myc antibody. row 4 represents Ponceau S stain. (D) 2 μM β-D-Ara*f* ABPs and ABP **7** incubated with GBA2 D677G mutant for 1 h (at 37 °C) or 24 h (at 4 °C) show the labelling efficiency towards GBA2 D677G mutant. (E) Structure of complex of *Tx*GH116 with **2** showing the electron density difference map calculated for the ligand and side chain of Glu441, contoured at 2.5 σ (0.275 electrons Å−3), and showing hydrogen bonds represented as dashed lines.

In vitro labelling across species *and in situ* labelling of β-D-Ara*f* cyclitol aziridine ABPs

GBA2 orthologs are highly conserved among different species. BLAST analysis revealed that human GBA2 shares 87% sequence identity and 93% similarity in the catalytic domain with murine GBA2 and 66% identity and 79% similarity with the zebrafish (Danio rerio) enzyme.[14] The reactivity of β-D-Ara*f* aziridine ABPs **3**-**5** with GBA2 orthologs in these was therefore evaluated. Homogenates of zebrafish larvae or mice brain were incubated with β-D-Ara*f* ABPs **3**-**5** or broad-spectrum β-glucosidase ABP **7** (Figure 4). As was seen for human cell extracts, β-D-Ara*f* ABPs **3**-**5** selectively label GBA2 also in these species whereas ABP **7** showed cross-reactivity towards GBA1.

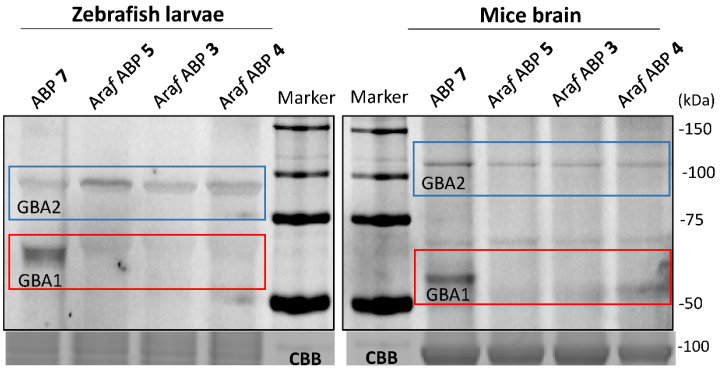

Figure 4. β-D-Ara*f* aziridine ABPs selectively label GBA2 orthologues in different species. Cyclophellitol aziridine ABP **7** (1 µM) and β-D-Ara*f* ABPs (ABP **3** at 1 µM and ABP **4** and **5** at 2.5 µM) were incubated with homogenates of zebrafish larvae and mice brain tissue for 1 h at 37 °C.

As the next research objective, experiments were done to establish whether active GBA2 molecules could be detected and identified in human cells using the β-D-Ara*f* aziridine ABPs. For this purpose, HEK293T cells with endogenous GBA1 and overexpressed GBA2/GBA3 were treated with varying concentrations of β-D-Ara*f* aziridine ABPs **3**-**5** for 1 h, after which the cells were harvested and washed multiple times prior to lysis. The lysates were then denatured, their protein content separated by SDS-PAGE and the resulting wet gel slabs scanned for fluorescence. In this way it was observed that all three β-D-Ara*f* ABPs **3**-**5** enter intact cells where they react with endogenous, and given the >24 h lifetime, newly synthesized GBA2 (Figure 5A, Figure S8 A, B). BODIPY tagged ABPs **3** and **4** proved to be the most effective GBA2 probes in these experiments and inactivate GBA2 almost completely at 100 nM final concentration.

To address the concern that the ABPs attach to the cell surface and subsequently *in vitro* label GBA2 following cell lysis, a non-tagged GBA2 inhibitor was added to the lysis buffer. The presence of high concentrations of cyclophellitol (**CP**) or cyclophellitol aziridine ABP **8**, both potent human GBA1 and GBA2 inactivators, did not diminish GBA2 labelling efficiency by ABP **4** (Figure 5B), thus indicating that these ABPs indeed labelled GBA2 *in situ*. Importantly, the GBA2 selectivity of β-D-Ara*f* ABPs **3**-**5** was maintained during *in situ* labelling of wild-type HEK293T cells (Figure S9). GBA1 labelling only occurred when using a high concentration (500 nM) and longer incubation time (2.5 h) for ABP **5**, while ABP **3** and **4** did not visibly label GBA1 at these conditions (Figure 5B and Figure S9). Even incubation for 24 h gave similar results: ABPs **3** and **4** still selectively labelled GBA2 at 10 nM, and only slight concomitant GBA1 labelling at higher concentrations was observed (Figure S10). Selective GBA2 labelling by ABPs **3** and **4** finally was also observed in human retinal pigment epithelial-1 cells (Figure 5C).

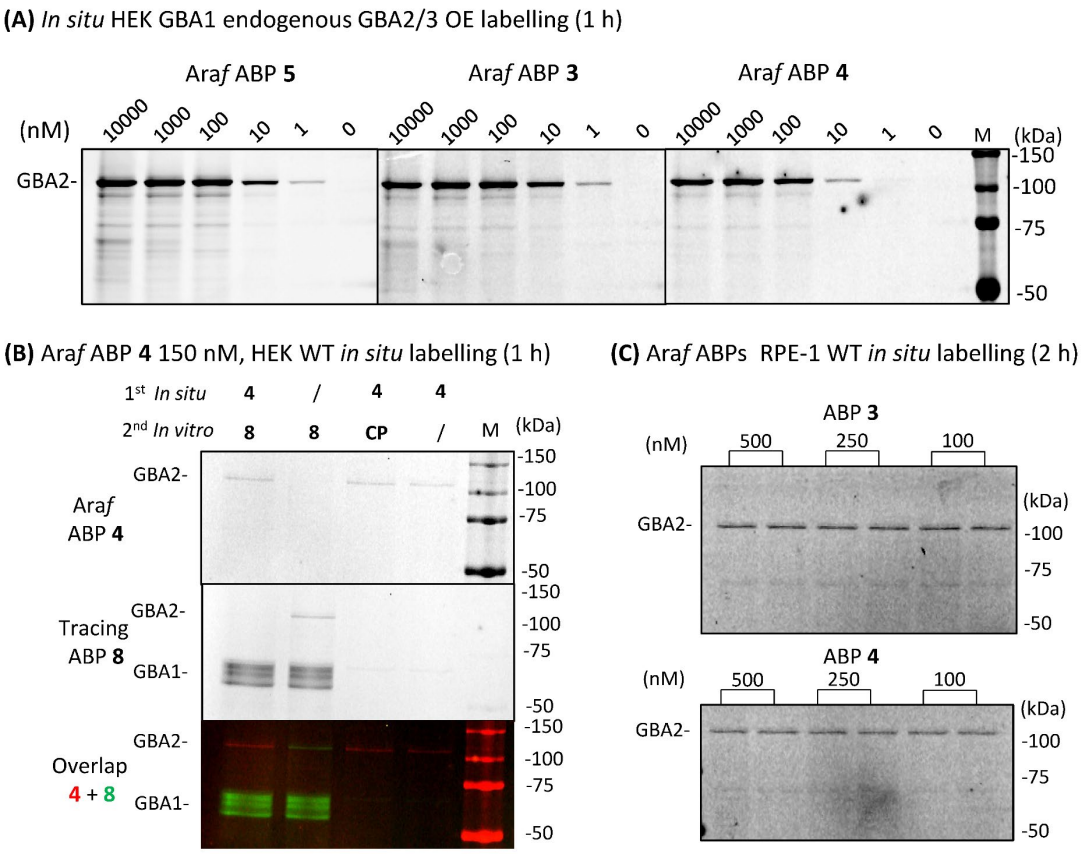

Figure 5. Treating intact cells with β-D-Ara*f* ABPs labels GBA2 *in situ*. (A) Labelling of β-D-Ara*f* ABPs in intact HEK293T cells (GBA1 endogenous and GBA2/3 overexpression) at varying concentrations for 1 h *in situ*. (B) Wild-type HEK293T cells treated with 150 nM ABP **4** *in situ* for 1 h, followed by adding lysis buffer containing ABP **8** (1 µM final concentration with 1% DMSO final concentration), or cyclophellitol (**CP**, 1 µM final concentration with 1% DMSO final concentration), or the blank ('/') 1% DMSO (final concentration) for ABPP analysis. (C) ABP **3** and **4** labelling of GBA2 in intact wild-type human retinal pigment epithelial-1 (RPE-1) cells.

Localization of GBA2 with an β-D-Ara*f* cyclitol aziridine ABP

As the final set of experiments, red fluorescent ABP **4** was used to study the localization of GBA2 in HEK293T cells. After incubation with 50 nM ABP **4** for 2 h, the samples were fixed and also stained with a green-fluorescent anti-GBA1-antibody in order to observe the difference in localization between GBA1 and GBA2. Confocal microscopy of wild-type (WT) HEK293T cells showed an unambiguous staining for GBA1 with a distinct perinuclear lysosomal distribution pattern. However, no clear signals for ABP **4** modified proteins were observed (Figure 6). Attention was therefore redirected to the use of GBA2 overexpression (OE) cells and GBA1/GBA2 knockout (KO) + GBA2 OE cells.[19,31] These cells did present clear GBA2 staining, which is localized to the cell membrane (Figure 6). As well, no overlap is observed between red fluorescence (localization of GBA2-selective ABP **4**) and green fluorescence (localization of GFP-tagged anti-GBA1), indicating that GBA2 resides in subcellular compartments distinct from those in which GBA1 resides. To confirm the selective staining of GBA2, cells overexpressing GBA2 were pre-treated with either the selective GBA1 inhibitor **21**[32] or the GBA1/GBA2 inhibitor **22**[35]. Confocal microscopy showed no change in the staining of GBA2 after pre-treatment with the GBA1 specific inhibitor **21**, however the signal of GBA2 was completely abrogated by prior treatment with the dual target inhibitor **22** (Figure S11B).

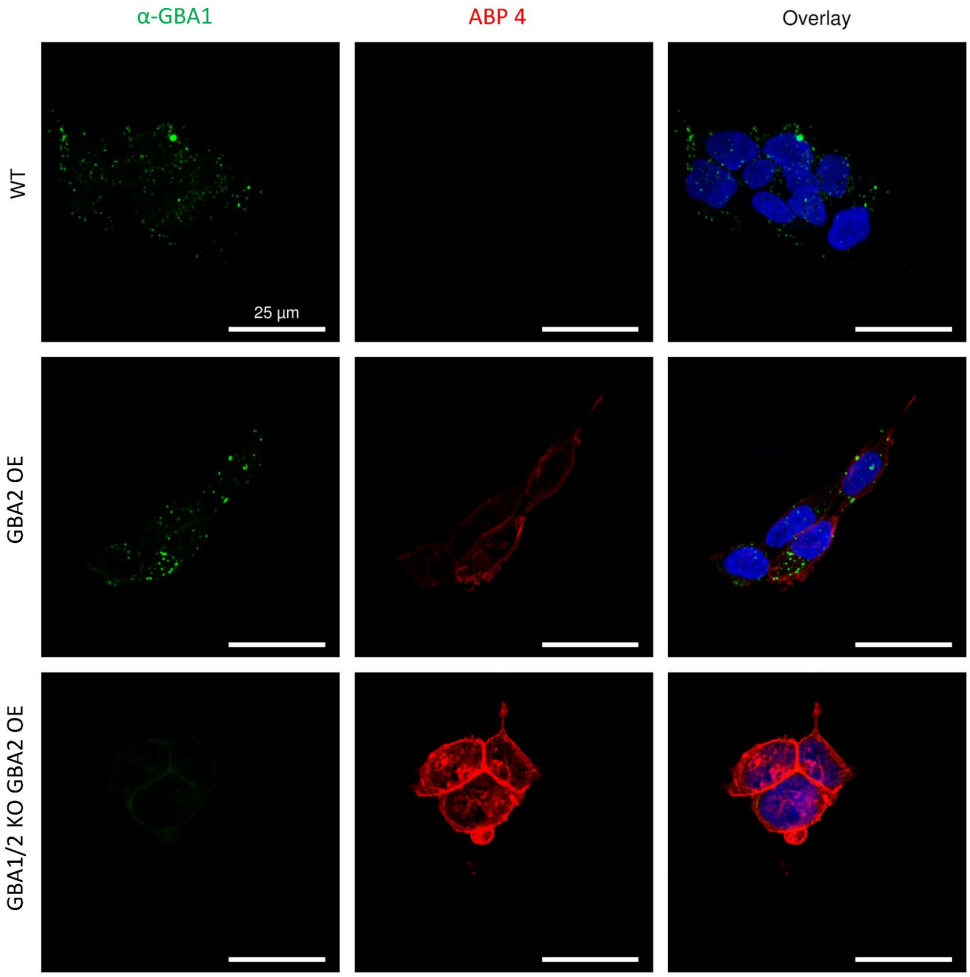

Figure 6. Confocal fluorescence microscopy of GBA1 and GBA2 as detected by red fluorescent β-D-Ara*f* aziridine **4** and green fluorescent anti-GBA1-antibody with Alexa Fluor® 647 conjugation. Used were different HEK293T cells: HEK293T wild-type (WT), GBA2 overexpression (OE), and GBA1/GBA2 knock out (KO) with GBA2 overexpression (OE). Cells were treated with 50 nM β-D-Ara*f* aziridine **4** (red) for 2 h. After fixation all cells were stained for GBA1 using an anti-GBA1-antibody (green) and nuclei were stained with 10 µg/ml DAPI (blue).

Discussion

GBA2 attracts increasing attention given its potential role in pathophysiological mechanisms in a variety of human diseases. While the catalytic machinery, the mode of action and the substrate specificity of the enzyme has now been firmly established, little is known about its physiological role and even its subcellular localization is a matter of debate. The acquisition of such knowledge is hampered by the absence of cell-permeable, GBA2-selective chemical probes, comparable to the counterpart developed for the selective visualization of active GBA1 in living cells.[30,36-38] The work described here was aimed to rectify this situation. Screening of a library of activity-based glycosidase probes led to the discovery of fluorescent β-D-Ara*f* cyclitol aziridines that selectively label GBA2 both *in vitro* and in intact cells. The labelling occurs through mechanism-based, covalent and irreversible inhibition of the ABP and is abolished by mutagenesis of the catalytic nucleophile. GBA2 labelling of cells combined with fluorescence microscopy clearly shows that GBA2, in contrast to GBA1, is not located in lysosomes. While labelled GBA2 is easily detected in cells overexpressing the enzyme, intensity of the fluorescent signal is relatively weak in wild type cells, and future use of more advanced fluorescence microscopy (for instance, including spectral imaging and use of a supersensitive camera with higher quantum yield) may improve detection of native GBA2. It should be kept in mind that

disperse distribution of GBA2 among membranes, contrary to the intrinsic concentration of GBA1 molecules in lysosomes, does not favor detection by simple fluorescence microscopy.

The observed high affinity and selectivity of β-D-Ara*f* cyclophellitol aziridines equipped with a hydrophobic fluorescent tag for labelling GBA2 is quite remarkable. A very recent publication by Shimokawa and coworkers[39] reports that a GH116 exo-β-D-arabinofuranosidase from *Microbacterium arabinogalactanolyticum* termed ExoMA2 shows similarities in structure to that of the GH116 β-glucosidase from *Thermoanaerobacterium xylanolyticum* (TxGH116). Both enzymes have a two-domain structure consisting of N-terminal β-sandwich and C-terminal (α/α) 6-barrel domains, the latter being the catalytic domain. The two catalytic residues, as well as several other residues in the active site pocket are conserved, but substrate recognition at subsite −1 differs. Given the similarities in the catalytic pocket, the catalytic residues and even the transglycosylation abilities[19,39,40] of the three enzymes, it is perhaps not surprising that β-D-Ara*f* cyclitol aziridines bind well to the GBA2 active site.

In conclusion, β-D-Ara*f* aziridine ABPs were identified as a new class of GBA2 selective ABPs. The newly described ABPs allow to specifically monitor GBA2 and act as specific GBA2 suicide inhibitors to selectively inactivate GBA2. The β-D-arabinofuranosyl cyclophellitol aziridine ABPs are novel tools for the study of the intriguing enzyme GBA2, and the development of GBA2 selective inhibitors based on the β-D-Ara*f* cyclophellitol scaffold is warranted in the future.

Experimental procedures

Materials

Recombinant human GBA1 (rhGBA1, Imiglucerase) was kindly provided by Sanofi Genzyme (Cambridge, MA, USA). HEK293T (CRL-3216™) cells and RPE-1 (CRL-4000™) cells were purchased from ATCC (Manassas, VA, USA). 4-Methylumbelliferyl-β-D-glucopyranoside was purchased from Glycosynth (Warrington Cheshire, UK). Polytron PT 1300D sonicator (Kinematica, Luzern, Switzerland) and potassium phosphate buffer (K_2HPO_4-KH_2PO_4, 25 mM, pH 6.5, supplemented with protease inhibitor cocktail (EDTA-free, Roche, Basel, Switzerland) and 0.1% (v/v) Triton X-100 and) were used for lysing cells and homogenizing zebrafish larvae and mice tissues. Harvested cells (cell pellets), cell lysates and tissue homogenates not used directly were stored at -80 °C. Protein concentration was measured using the Pierce BCA assay kit (Thermo Fisher Scientific, Waltham, MA, USA).

Cell culture

HEK293T cells were cultured in DMEM medium (Sigma-Aldrich), supplied with 10% (v/v) FCS, 0.1% (w/v) penicillin/streptomycin and 1% (v/v) Glutamax, at 37 °C under 7% CO_2. RPE-1 cells were cultured in HAMF12-DMEM medium (Sigma Aldrich), supplied with 10% (v/v) FCS, 0.1% (w/v) penicillin/streptomycin and 1% (v/v) Glutamax, at 37 °C under 5% CO_2.

Generation of cells genetically modified in β-glucosidase expression

GBA1/GBA2 knockout (KO) HEK293T cells, GBA1/GBA2 KO HEK293T cells with either GBA2 overexpression (OE) or GBA3 overexpression, and HEK293T cells expressing all cellular β-glucosidases (containing endogenous GBA1 and overexpressed GBA2 and GBA3) were generated as described in Chapter 2.

Cell lysis

HEK293T and RPE-1 cells were cultured with the method described above to 80-90% confluency, and were isolated, washed with Dulbecco's phosphate buffered saline (PBS), subsequently collected and lysed as the method described in Chapter 2 which were adapted from the literature.[41]

4MU fluorogenic substrate assay for determination of enzyme activity and apparent IC_{50}

4MU fluorogenic substrate assays (using isolated recombination human GBA1 or lysates of HEK293T cells) were conducted in 96-well plates at 37 °C. Assay procedures and conditions for measuring enzyme activity and apparent IC_{50} of each enzyme (rhGBA1, GBA2, or GBA3) are the same as previously described in Chapter 2. In brief, enzymes were diluted with McIlvaine buffer (150 mM citric acid-Na_2HPO_4, at the appropriate pH for each enzyme), to a final volume of 25 µL with or without inhibitors. For enzyme activity measurement, samples were incubated with 100 µL 4-methylumbelliferyl-β-D-glucopyranoside substrates diluted in McIlvaine buffer for 30 min. For apparent IC_{50} measurement, enzymes were incubated with inhibitor diluted in McIlvaine buffer for 30 min or 3 h, followed by incubation with 100 µL 4-methylumbelliferyl-β-D-glucopyranoside substrates for 30 min. After stopping the enzyme reaction with 200 µL 1M NaOH-glycine (pH 10.3), 4-methylumbelliferone fluorescence was measured with a fluorimeter LS55 (Perkin Elmer, Waltham, MA, USA). Enzyme activities and apparent IC_{50} values were determined by subtraction of the background signal (measured for incubations without enzyme), as previously described.[42] The IC_{50} value was calculated using Graphpad Prism 9.0 with the Nonlinear regression (curve fit) - [Inhibitor] vs. response - Variable slope (four parameters) equation.

Activity-based protein profiling (ABPP) with SDS-PAGE

Samples containing GBA1, GBA2 or GBA3 (see the exact constitution of these samples as described in the specific case) were incubated with fluorescent ABPs at optimum conditions at 37 °C for 30 min (if not otherwise stated) as described in Chapter 2. The total sample volume was 20–40 µL with a 0.5–1% final concentration of DMSO in the appropriate pH McIlvaine buffer (150 mM). For assessing the reactivity of arabinofuranose-configured cyclitol ABPs towards β-glucosidases, lysates of HEK293T cells expressing endogenous GBA1 and overexpressed GBA2/GBA3 were incubated with varying concentration of ABP in McIlvaine buffer (150 mM, pH 6.0). After incubation with ABP, samples were subjected to SDS-PAGE and fluorescence scanning as described in Chapter 2. Wet gel slabs were imaged using a Typhoon FLA 9500 scanner (GE Healthcare) at λ_{EX} 473 nm and λ_{EM} ≥ 510 nm for BODIPY green fluorescence; at λ_{EX} 532 nm and λ_{EM} ≥ 575 nm for the BODIPY red fluorescence; at λ_{EX} 635 nm and λ_{EM} ≥ 665 nm for Cy5 fluorescence. Afterwards, the wet gel slab was stained by Coomassie brilliant blue (CBB) G250 or R250 for loading control of proteins.

β-Glucosidase inactivation visualized by competitive ABPP with SDS-PAGE

In general, samples containing GBA1, GBA2 or GBA3 (see the exact constitution of these samples described below) are first incubated (*in vitro* or *in situ*) with the compounds, subsequently, the fluorescent readout ABPs were added and incubated with mixture to reveal the residual enzymes that were not inactivated by the inhibitor compound.

To Figure S12, lysate of HEK293T cells expressing all cellular β-glucosidases were first incubated with compound **6** for 3 h at 37°C (*in vitro*), after which readout ABP **7** was added and incubated for 30 min at 37 °C (*in vitro*) to reveal the residual active β-glucosidases, following the procedures described above for SDS-PAGE and fluorescence scanning to visualize the outcome. To Figure S8B, intact living HEK293T cells expressing all cellular β-glucosidases were first incubated with fluorescent ABP **3**-**5** (*in situ*) for 24h at 37°C under 7% CO_2, then cells were harvest and lysed as description in cell lysis. Subsequently, readout ABP (one of **7**-**9**) was added, and same procedures described above for outcome visualization were conducted to reveal the active β-glucosidases not occupied by ABP **3**-**5**. Of note, a fluorescent readout ABP (**7**-**9**) with different scanning wavelength from ABP (**3**-**5**) should be chosen. For example, if ABP **3** with BODIPY-green tag is first used to inactivate β-glucosidases, the readout ABP should be ABP **7** with Cy5 tag or ABP **9** with BODIPY-red tag.

To obtain competitive ABPP quantified IC_{50} values, the ABP-emitted fluorescence of the read out ABP was quantified by ImageQuant (GE Healthcare, Chicago, IL, USA) and calculated with Graphpad Prism 9.0 using Analyze – Nonlinear regression (curve fit) – One phase association.

Irreversibility evaluation by competition with irreversible ABP

The irreversibility of enzyme inhibition was evaluated as below (Figure S6A). Lysates of GBA1/GBA2 KO HEK293T with GBA2 OE were used. A total of 60 µg lysate was incubated with or without 1 µM β-D-Ara*f* cyclitol aziridines **2**-**4** for 1 h at 37 °C, a part of the lysates was taken and used for parallel activity measurements using the 4MU-β-D-Glc fluorogenic substrate assay. Subsequently, the lysate mixtures were washed by passing through Zeba™ spin desalting columns with 40k MWCO (Thermo Scientific) to remove excess compounds. The washing was repeated every 2 h, with 3 washes conducted in total, during which the lysate was kept on ice or at 4 °C. After the last washing step, the same volume of lysates was taken and incubated with 1 µM β-glucosidase ABP **7**, over 30 min at 37 °C, or over 24 h or 48 h at 4 °C. Then the competition results were revealed by SDS-PAGE and in-gel fluorescence scanning as described above. Parallel activity measurement results show GBA2 activity recovery after desalting washing (Figure S6B).

Stability of β-D-Ara*f* aziridine binding towards GBA2

In Figure S6C, A total of 90 µg GBA2 (lysates of GBA1/GBA2 KO HEK293T with GBA2 OE) in potassium phosphate buffer was diluted with 60 µL McIlvaine buffer (150 mM, pH 6.0) and incubated with or without 1 µM β-D-Ara*f* aziridine compound **2**-**5** for 1 h at 37 °C. Thereafter, the total 100 µL sample was passed through a desalting column as described above. To assess the activity of GBA2 bound with the β-D-Ara*f* compound **2**-**5**, all samples were kept at 4 °C until GBA2 activity was measured by incubation with 4MU-β-D-Glc at time points 0.5 h, 24 h and 96 h and subsequent measurement of emerging fluorescence. The GBA2 activity assays were performed with 10 µL sample in triplicate, and the activity of GBA2 incubated without inhibitors was used as a control.

Reactivity of β-D-Ara*f* aziridines towards GBA2 mutants

For overexpression of GBA2 mutants, HEK293T GBA1/GBA2 KO cells were used. GBA2-E527G, GBA2-D677G, or GBA2- E527G/D677G double mutants containing a myc tag were generated as described previously for COS-7 cells.[17] Next, 500 nM β-D-Ara*f* cyclitol aziridine ABP **3**-**5** or cyclophellitol-aziridine ABP **7** were incubated with the corresponding lysates for 30 min at 37 °C, followed by SDS-PAGE and fluorescence scanning as described in ABPP. Subsequently, proteins in the wet gel slabs were transferred to nitrocellulose membranes for Western blotting. Ponceau S staining was used to show loading control of proteins. Primary antibody used was Mouse anti myc (α-myc, Bioke). Secondary antibodies, donkey anti mouse with Alexa 488 (Invitrogen) or goat anti mouse with Alexa 532 (Invitrogen) were used to visualize GBA2 mutants with the myc tag.

Reactivity of β-D-Ara*f* aziridines towards GBA2 orthologue in other species

β-D-Ara*f* aziridine ABP **3**-**5** or ABP **7** was incubated with homogenates of zebrafish (*Danio rerio*) larvae or mice brain for 1 h at 37 °C. The homogenates were obtained as follows. Zebrafish larvae were kept at a constant temperature of 28.5 °C and raised in egg water (60 µg L-1 sea salt, Sera Marin) for 5 days, larvae were collected and sacrificed for making homogenates, a total 10-20 µg larvae homogenates were used for ABPP. Extracts of mouse brain were obtained from existing mice extraction stocks that were stored at –20 °C; a total of 10-20 µg mouse brain homogenate was used. The zebrafish homogenate was passed through a desalting column (in the same way as described for the irreversibility evaluation above) to remove interference from biological pigments when scanning at λEX 473 nm and λEM ≥ 510 nm for BODIPY green fluorescence.

***In situ* intact cell permeability assays**

Confluent HEK293T cells expressing human endogenous GBA1 and overexpressed GBA2/GBA3, wild-type HEK293T cells or wild-type human retinal pigment epithelial-1 (RPE-1) cells were cultured in 12-well plates for duplicates or triplicates with (or without) compounds (**3-5**) for the described incubation times using the conditions as described for the cell culture. The cells were harvested and lysed as described in the cell lysis method. After determination of the protein concentration by BCA assay, the lysates were adjusted to 10 µL by addition of potassium phosphate buffer in order to normalize the amount of protein loaded (to 10-25 µg total protein per measurement) and subjected to ABPP as described above.

***In situ* visualization of GBA2 using confocal microscopy**

HEK293T wild-type (WT), GBA1 endogenous and GBA2 overexpression (GBA2 OE), or GBA1/GBA2 knockout (KO) GBA2 overexpression (GBA1/GBA2 KO GBA2 OE) cells were cultured as described in cell culture.[31,43] Cells were grown to approximately 75% confluency on Ø15 mm glass coverslips coated with 0.1 mg/ml poly-D-Lysine. Samples were pretreated for 16 h with 100 nM of a GBA1 inhibitor (**21**[32], 0.5% DMSO), 500 nM of a GBA1 and GBA2 inhibitor (**22**[35], 0.5% DMSO) or with 0.5% DMSO alone. GBA2 was

subsequently incubated by the addition of 50 nM ABP **4** (BODIPY-red) to cells for 2 h at 37 °C with 5% CO_2. Unbound probe was washed away with PBS and cells were fixed with 4% paraformaldehyde (Alfa Aesar)/PBS for 15 min at RT. After fixation the cells were washed with PBS and directly permeabilized with 0.1% Tween20 (Sigma-Aldrich)/TBS for 30 min at RT. After gentle washing in PBS, the samples were blocked using 3% (w/v) BSA (Sigma-Aldrich)/PBS for 30 min at RT. Immunofluorescence staining was performed with mouse-αnti-GBA1 (8E4, generated as described in the literature[44] 1:250 in 3% BSA-PBS and visualized with a donkey-αnti-mouse-Alexa647 (Molecular Probes) 1:1000 in 3% BSA-PBS. Nuclei were stained with 10 µg/ml DAPI (Sigma-Aldrich). Afterwards the samples were mounted on ProLong Diamond (Molecular Probes) and imaged on a Nikon Eclipse Ti2 confocal microscope with a 100x/1.49 Numerical Aperture SR HP Apo TIRF oil immersion objective equipped with a PMTs detector.

Expression, purification and crystallization of *Tx*GH116

A construct consisting of *Tx*GH116Δ1-18 cloned into pET30a was transformed into *E. coli* BL21(DE3) and used for the expression of *Tx*GH116 and its purification based on the method described.[16] Purified *Tx*GH116 at 1 mg/ml in 20 mM Tris–HCl pH 8.0, 150 mM NaCl was crystalized in a sitting drop plate, in a 2:1 ratio to the well solution, which consisted of 20 % (w/v) polyethylene glycol 3000, 100 mM ammonium sulfate, 0.1 M 2-(*N*-morpholino) ethanesulfonic acid pH 6.0. A crystal was soaked by the addition of a 10 mM solution of 8-azidooctyl-β-D-arabinofuranosyl cyclitol aziridine **2** dissolved in water to a final concentration of 3.3 mM in the drop and fished after 68 hours into liquid nitrogen without additional cryoprotection.

Data collection and refinement

Data were collected at beamline io4 at the Diamond Light Source (UK), processed using DIALS[45] and scaled with *AIMLESS*[46]. There are 2 molecules per asymmetric unit and the space group is $P2_12_12_1$. The structure was solved using *Phaser*[47] with PDB entry 5BVU as the model, and refined using REFMAC5[48] interspersed with rounds of model building in *Coot*[49]. The ligand was built and dictionary restraints generated using *AceDRG*[50]. The programs were run through the *CCP*4*I*2[51] graphical interface. Data collection and refinement statistics are given in Table S2.

References

1. E. Drula, M. L. Garron, S. Dogan, V. Lombard, B. Henrissat and N. Terrapon, The carbohydrate-active enzyme database: functions and literature, *Nucleic Acids Res.*, 2022, **50**, D571-D577.
2. S. van Weely, M. Brandsma, A. Strijland, J. M. Tager and J. M. Aerts, Demonstration of the existence of a second, non-lysosomal glucocerebrosidase that is not deficient in Gaucher disease, *Biochim. Biophys. Acta.*, 1993, **1181**, 55-62.
3. S. Sultana, J. Reichbauer, R. Schule, F. Mochel, M. Synofzik and A. C. van der Spoel, Lack of enzyme activity in GBA2 mutants associated with hereditary spastic paraplegia/cerebellar ataxia (SPG46), *Biochem. Biophys. Res. Commun.*, 2015, **465**, 35-40.
4. E. Martin, R. Schule, K. Smets, A. Rastetter, A. Boukhris, J. L. Loureiro, M. A. Gonzalez, E. Mundwiller, T. Deconinck, M. Wessner, L. Jornea, A. C. Oteyza, A. Durr, J. J. Martin, L. Schols, C. Mhiri, F. Lamari, S. Zuchner, P. De Jonghe, E. Kabashi, A. Brice and G. Stevanin, Loss of function of glucocerebrosidase GBA2 is responsible for motor neuron defects in hereditary spastic paraplegia, *Am. J. Hum. Genet.*, 2013, **92**, 238-244.
5. M. Gatti, S. Magri, D. Di Bella, E. Sarto, F. Taroni, C. Mariotti and L. Nanetti, Spastic paraplegia type 46: novel and recurrent GBA2 gene variants in a compound heterozygous Italian patient with spastic ataxia phenotype, *Neurol. Sci.*, 2021, **42**, 4741-4745.
6. M. A. Woeste, S. Stern, D. N. Raju, E. Grahn, D. Dittmann, K. Gutbrod, P. Dormann, J. N. Hansen, S. Schonauer, C. E. Marx, H. Hamzeh, H. G. Korschen, J. M. Aerts, W. Bonigk, H. Endepols, R. Sandhoff, M. Geyer, T. K. Berger, F. Bradke and D. Wachten, Species-specific differences in nonlysosomal glucosylceramidase GBA2 function underlie locomotor dysfunction arising from loss-of-function mutations, *J. Biol. Chem.*, 2019, **294**, 3853-3871.
7. Biogen, June 6, 2022, ''Biogen and Alectos Therapeutics announce license and collaboration agreement for AL01811, a novel GBA2 inhibitor for the potential treatment of Parkinson's disease'', https://investors.biogen.com/news-releases/news-release-details/biogen-and-alectos-therapeutics-announce-license-and.
8. Y. Yildiz, H. Matern, B. Thompson, J. C. Allegood, R. L. Warren, D. M. Ramirez, R. E. Hammer, F. K. Hamra, S. Matern and D. W. Russell, Mutation of beta-glucosidase 2 causes glycolipid storage disease and impaired male fertility, *J. Clin. Invest.*, 2006, **116**, 2985-2994.
9. R. G. Boot, M. Verhoek, W. Donker-Koopman, A. Strijland, J. van Marle, H. S. Overkleeft, T. Wennekes and J. M. Aerts, Identification of the non-lysosomal glucosylceramidase as beta-glucosidase 2, *J. Biol. Chem.*, 2007, **282**, 1305-1312.
10. B. Cobucci-Ponzano, V. Aurilia, G. Riccio, B. Henrissat, P. M. Coutinho, A. Strazzulli, A. Padula, M. M. Corsaro, G. Pieretti, G. Pocsfalvi, I. Fiume, R. Cannio, M. Rossi and M. Moracci, A new archaeal beta-glycosidase from Sulfolobus solfataricus: seeding a novel retaining beta-glycan-specific glycoside hydrolase family along with the human non-lysosomal glucosylceramidase GBA2, *J. Biol. Chem.*, 2010, **285**, 20691-20703.
11. S. Pengthaisong, B. Piniello, G. J. Davies, C. Rovira and J. R. Ketudat Cairns, Reaction mechanism of glycoside hydrolase family 116 utilizes perpendicular protonation, *ACS Catal.*, 2023, **13**, 5850-5863.
12. G. Y. Dai, J. Yin, K. E. Li, D. K. Chen, Z. Liu, F. C. Bi, C. Rong and N. Yao, The Arabidopsis AtGCD3 protein is a glucosylceramidase that preferentially hydrolyzes long-acyl-chain glucosylceramides, *J. Biol. Chem.*, 2020, **295**, 717-728.
13. L. T. Lelieveld, M. Mirzaian, C.-L. Kuo, M. Artola, M. J. Ferraz, R. E. A. Peter, H. Akiyama, P. Greimel, R. J. B. H. N. van den Berg, H. S. Overkleeft, R. G. Boot, A. H. Meijer and J. M. Aerts, Role of μ-glucosidase 2 in aberrant glycosphingolipid metabolism: model of glucocerebrosidase deficiency in zebrafish, *J. Lipid Res.*, 2019, **60**, 1851-1867.
14. S. Sultana, N. Y. Truong, D. B. Vieira, J. G. Wigger, A. M. Forrester, C. J. Veinotte, J. N. Berman and A. C. van der Spoel, Characterization of the zebrafish homolog of beta-glucosidase 2: a target of the drug Miglustat, *Zebrafish*, 2016, **13**, 177-187.

15. A. R. Marques, J. Aten, R. Ottenhoff, C. P. van Roomen, D. Herrera Moro, N. Claessen, M. F. Vinueza Veloz, K. Zhou, Z. Lin, M. Mirzaian, R. G. Boot, C. I. De Zeeuw, H. S. Overkleeft, Y. Yildiz and J. M. Aerts, Reducing GBA2 activity ameliorates neuropathology in Niemann-Pick type C mice, *PLoS One*, 2015, **10**, e0135889.
16. R. Charoenwattanasatien, S. Pengthaisong, I. Breen, R. Mutoh, S. Sansenya, Y. Hua, A. Tankrathok, L. Wu, C. Songsiriritthigul, H. Tanaka, S. J. Williams, G. J. Davies, G. Kurisu and J. R. Cairns, Bacterial beta-glucosidase reveals the structural and functional basis of genetic defects in human glucocerebrosidase 2 (GBA2), *ACS Chem. Biol.*, 2016, **11**, 1891-1900.
17. W. W. Kallemeijn, M. D. Witte, T. M. Voorn-Brouwer, M. T. Walvoort, K. Y. Li, J. D. Codée, G. A. van der Marel, R. G. Boot, H. S. Overkleeft and J. M. Aerts, A sensitive gel-based method combining distinct cyclophellitol-based probes for the identification of acid/base residues in human retaining beta-glucosidases, *J. Biol. Chem.*, 2014, **289**, 35351-35362.
18. H. G. Korschen, Y. Yildiz, D. N. Raju, S. Schonauer, W. Bonigk, V. Jansen, E. Kremmer, U. B. Kaupp and D. Wachten, The non-lysosomal beta-glucosidase GBA2 is a non-integral membrane-associated protein at the endoplasmic reticulum (ER) and Golgi, *J. Biol. Chem.*, 2013, **288**, 3381-3393.
19. A. R. Marques, M. Mirzaian, H. Akiyama, P. Wisse, M. J. Ferraz, P. Gaspar, K. Ghauharali-van der Vlugt, R. Meijer, P. Giraldo, P. Alfonso, P. Irun, M. Dahl, S. Karlsson, E. V. Pavlova, T. M. Cox, S. Scheij, M. Verhoek, R. Ottenhoff, C. P. van Roomen, N. S. Pannu, M. van Eijk, N. Dekker, R. G. Boot, H. S. Overkleeft, E. Blommaart, Y. Hirabayashi and J. M. Aerts, Glucosylated cholesterol in mammalian cells and tissues: formation and degradation by multiple cellular beta-glucosidases, *J. Lipid Res.*, 2016, **57**, 451-463.
20. H. Akiyama, M. Ide, Y. Nagatsuka, T. Sayano, E. Nakanishi, N. Uemura, K. Yuyama, Y. Yamaguchi, H. Kamiguchi, R. Takahashi, J. M. Aerts, P. Greimel and Y. Hirabayashi, Glucocerebrosidases catalyze a transgalactosylation reaction that yields a newly-identified brain sterol metabolite, galactosylated cholesterol, *J. Biol. Chem.*, 2020, **295**, 5257-5277.
21. T. Cox, R. Lachmann, C. Hollak, J. M. Aerts, S. van Weely, M. Hrebicek, F. Platt, T. Butters, R. Dwek, C. Moyses, I. Gow, D. Elstein and A. Zimran, Novel oral treatment of Gaucher's disease with N-butyldeoxynojirimycin (OGT 918) to decrease substrate biosynthesis, *Lancet*, 2000, **355**, 1481-1485.
22. T. M. Cox, J. M. Aerts, G. Andria, M. Beck, N. Belmatoug, B. Bembi, R. Chertkoff, S. Vom Dahl, D. Elstein, A. Erikson, M. Giralt, R. Heitner, C. Hollak, M. Hrebicek, S. Lewis, A. Mehta, G. M. Pastores, A. Rolfs, M. C. Miranda, A. Zimran and Advisory Council to the European Working Group on Gaucher, The role of the iminosugar N-butyldeoxynojirimycin (miglustat) in the management of type I (non-neuronopathic) Gaucher disease: a position statement, *J. Inherit Metab. Dis.*, 2003, **26**, 513-526.
23. M. Pineda, M. Walterfang and M. C. Patterson, Miglustat in Niemann-Pick disease type C patients: a review, *Orphanet J. Rare Dis.*, 2018, **13**, 140.
24. P. K. Mistry, J. Liu, L. Sun, W. L. Chuang, T. Yuen, R. Yang, P. Lu, K. Zhang, J. Li, J. Keutzer, A. Stachnik, A. Mennone, J. L. Boyer, D. Jain, R. O. Brady, M. I. New and M. Zaidi, Glucocerebrosidase 2 gene deletion rescues type 1 Gaucher disease, *Proc. Natl. Acad. Sci. U. S. A.*, 2014, **111**, 4934-4939.
25. D. G. Burke, A. A. Rahim, S. N. Waddington, S. Karlsson, I. Enquist, K. Bhatia, A. Mehta, A. Vellodi and S. Heales, Increased glucocerebrosidase (GBA) 2 activity in GBA1 deficient mice brains and in Gaucher leucocytes, *J. Inherit Metab. Dis.*, 2013, **36**, 869-872.
26. J. K. Amory, C. H. Muller, S. T. Page, E. Leifke, E. R. Pagel, A. Bhandari, B. Subramanyam, W. Bone, A. Radlmaier and W. J. Bremner, Miglustat has no apparent effect on spermatogenesis in normal men, *Hum. Reprod.*, 2007, **22**, 702-707.
27. H. S. Overkleeft, G. H. Renkema, J. Neele, P. Vianello, I. O. Hung, A. Strijland, A. M. van der Burg, G. J. Koomen, U. K. Pandit and J. M. Aerts, Generation of specific deoxynojirimycin-type inhibitors of the non-lysosomal glucosylceramidase, *J. Biol. Chem.*, 1998, **273**, 26522-26527.

28. W. W. Kallemeijn, K. Y. Li, M. D. Witte, A. R. Marques, J. Aten, S. Scheij, J. Jiang, L. I. Willems, T. M. Voorn-Brouwer, C. P. van Roomen, R. Ottenhoff, R. G. Boot, H. van den Elst, M. T. Walvoort, B. I. Florea, J. D. Codée, G. A. van der Marel, J. M. Aerts and H. S. Overkleeft, Novel activity-based probes for broad-spectrum profiling of retaining beta-exoglucosidases in situ and in vivo, *Angew. Chem. Int. Ed.*, 2012, **51**, 12529-12533.
29. L. Wu, Z. Armstrong, S. P. Schröder, C. de Boer, M. Artola, J. M. Aerts, H. S. Overkleeft and G. J. Davies, An overview of activity-based probes for glycosidases, *Curr. Opin. Chem. Biol.*, 2019, **53**, 25-36.
30. M. D. Witte, W. W. Kallemeijn, J. Aten, K. Y. Li, A. Strijland, W. E. Donker-Koopman, A. M. van den Nieuwendijk, B. Bleijlevens, G. Kramer, B. I. Florea, B. Hooibrink, C. E. Hollak, R. Ottenhoff, R. G. Boot, G. A. van der Marel, H. S. Overkleeft and J. M. Aerts, Ultrasensitive in situ visualization of active glucocerebrosidase molecules, *Nat. Chem. Biol.*, 2010, **6**, 907-913.
31. Q. Su, S. P. Schröder, L. T. Lelieveld, M. J. Ferraz, M. Verhoek, R. G. Boot, H. S. Overkleeft, J. M. Aerts, M. Artola and C. L. Kuo, Xylose-configured cyclophellitols as selective inhibitors for glucocerebrosidase, *Chembiochem*, 2021, **22**, 3090-3098.
32. M. Artola, C. L. Kuo, L. T. Lelieveld, R. J. Rowland, G. A. van der Marel, J. D. C. Codée, R. G. Boot, G. J. Davies, J. M. Aerts and H. S. Overkleeft, Functionalized cyclophellitols are selective glucocerebrosidase inhibitors and induce a bona fide neuropathic Gaucher model in zebrafish, *J. Am. Chem. Soc.*, 2019, **141**, 4214-4218.
33. O. Lopez Lopez, J. G. Fernandez-Bolanos, V. H. Lillelund and M. Bols, Aziridines as a structural motif to conformational restriction of azasugars, *Org. Biomol. Chem.*, 2003, **1**, 478-482.
34. D. E. Koshland, Stereochemistry and the mechanism of enzymatic reactions, *Biol. Rev.*, 1953, **28**, 416-436.
35. K. Y. Li, J. Jiang, M. D. Witte, W. W. Kallemeijn, W. E. Donker-Koopman, R. G. Boot, J. M. Aerts, J. D. Codée, G. A. van der Marel and H. S. Overkleeft, Exploring functional cyclophellitol analogues as human retaining beta-glucosidase inhibitors, *Org. Biomol. Chem.*, 2014, **12**, 7786-7791.
36. A. K. Yadav, D. L. Shen, X. Shan, X. He, A. R. Kermode and D. J. Vocadlo, Fluorescence-quenched substrates for live cell imaging of human glucocerebrosidase activity, *J. Am. Chem. Soc.*, 2015, **137**, 1181-1189.
37. M. C. Deen, C. Proceviat, X. Shan, L. Wu, D. L. Shen, G. J. Davies and D. J. Vocadlo, Selective fluorogenic beta-glucocerebrosidase substrates for convenient analysis of enzyme activity in cell and tissue homogenates, *ACS Chem. Biol.*, 2020, **15**, 824-829.
38. S. Zhu, M. C. Deen, Y. Zhu, P. A. Gilormini, X. Chen, O. B. Davis, M. Y. Chin, A. G. Henry and D. J. Vocadlo, A fixable fluorescence-quenched substrate for quantitation of lysosomal glucocerebrosidase activity in both live and fixed cells, *Angew. Chem. Int. Ed.*, 2023, DOI: 10.1002/anie.202309306, e202309306.
39. M. Shimokawa, A. Ishiwata, T. Kashima, C. Nakashima, J. Li, R. Fukushima, N. Sawai, M. Nakamori, Y. Tanaka, A. Kudo, S. Morikami, N. Iwanaga, G. Akai, N. Shimizu, T. Arakawa, C. Yamada, K. Kitahara, K. Tanaka, Y. Ito, S. Fushinobu and K. Fujita, Identification and characterization of endo-alpha-, exo-alpha-, and exo-beta-D-arabinofuranosidases degrading lipoarabinomannan and arabinogalactan of mycobacteria, *Nat. Commun.*, 2023, **14**, 5803.
40. S. Pengthaisong, Y. Hua and J. R. Ketudat Cairns, Structural basis for transglycosylation in glycoside hydrolase family GH116 glycosynthases, *Arch. Biochem. Biophys.*, 2021, **706**, 108924.
41. C. L. Kuo, E. van Meel, K. Kytidou, W. W. Kallemeijn, M. Witte, H. S. Overkleeft, M. Artola and J. M. Aerts, Activity-based probes for glycosidases: profiling and other applications, *Methods Enzymol.*, 2018, **598**, 217-235.
42. C. L. Kuo, W. W. Kallemeijn, L. T. Lelieveld, M. Mirzaian, I. Zoutendijk, A. Vardi, A. H. Futerman, A. H. Meijer, H. P. Spaink, H. S. Overkleeft, J. M. Aerts and M. Artola, In vivo inactivation of glycosidases by conduritol B epoxide and cyclophellitol as revealed by activity-based protein profiling, *FEBS J.*, 2019, **286**, 584-600.

43. D. Lahav, B. Liu, R. van den Berg, A. van den Nieuwendijk, T. Wennekes, A. T. Ghisaidoobe, I. Breen, M. J. Ferraz, C. L. Kuo, L. Wu, P. P. Geurink, H. Ovaa, G. A. van der Marel, M. van der Stelt, R. G. Boot, G. J. Davies, J. M. Aerts and H. S. Overkleeft, A fluorescence polarization activity-based protein profiling assay in the discovery of potent, selective inhibitors for human nonlysosomal glucosylceramidase, *J. Am. Chem. Soc.*, 2017, **139**, 14192-14197.
44. J. M. Aerts, W. E. Donker-Koopman, G. J. Murray, J. A. Barranger, J. M. Tager and A. W. Schram, A procedure for the rapid purification in high yield of human glucocerebrosidase using immunoaffinity chromatography with monoclonal antibodies, *Anal. Biochem.*, 1986, **154**, 655-663.
45. D. G. Waterman, G. Winter, R. J. Gildea, J. M. Parkhurst, A. S. Brewster, N. K. Sauter and G. Evans, Diffraction-geometry refinement in the DIALS framework, *Acta Crystallogr. D*, 2016, **72**, 558-575.
46. P. R. Evans and G. N. Murshudov, How good are my data and what is the resolution?, *Acta Crystallogr. D*, 2013, **69**, 1204-1214.
47. A. J. McCoy, R. W. Grosse-Kunstleve, P. D. Adams, M. D. Winn, L. C. Storoni and R. J. Read, Phaser crystallographic software, *J. Appl. Crystallogr.*, 2007, **40**, 658-674.
48. G. N. Murshudov, P. Skubak, A. A. Lebedev, N. S. Pannu, R. A. Steiner, R. A. Nicholls, M. D. Winn, F. Long and A. A. Vagin, REFMAC5 for the refinement of macromolecular crystal structures, *Acta Crystallogr. D*, 2011, **67**, 355-367.
49. P. Emsley, B. Lohkamp, W. G. Scott and K. Cowtan, Features and development of Coot, *Acta Crystallogr. D*, 2010, **66**, 486-501.
50. F. Long, R. A. Nicholls, P. Emsley, S. Graaeulis, A. Merkys, A. Vaitkus and G. N. Murshudov, AceDRG: a stereochemical description generator for ligands, *Acta Crystallogr. D*, 2017, **73**, 112-122.
51. L. Potterton, J. Agirre, C. Ballard, K. Cowtan, E. Dodson, P. R. Evans, H. T. Jenkins, R. Keegan, E. Krissinel, K. Stevenson, A. Lebedev, S. J. McNicholas, R. A. Nicholls, M. Noble, N. S. Pannu, C. Roth, G. Sheldrick, P. Skubak, J. Turkenburg, V. Uski, F. von Delft, D. Waterman, K. Wilson, M. Winn and M. Wojdyr, CCP4i2: the new graphical user interface to the CCP4 program suite, *Acta Crystallogr. D*, 2018, **74**, 68-84.

Appendix

Table S1. Apparent IC_{50} values (nM) of arabinofuranosyl cyclitol configured compounds as β-glucosidase inhibitors, determined by 4-MU-β-D-Glc fluorogenic substrate assays.

β-D-Ara*f*	GBA2 [a]	rhGBA1 [b]	GBA3 [c]
1 (aziridine)	> 50000	> 50000	> 50000
2 (octyl-azido)	630.0 ± 95.6	2730.0 ± 907.2	8149.6 ± 1425.8
3 (BODIPY green)	124.4 ± 4.9	4292.3 ± 157.1	>10000
4 (BODIPY red)	162.2 ± 34.7	1777.0 ± 71.0	> 10000
5 (Cy5)	263.7 ± 23.5	295.1 ± 35.3	1518.7 ± 159.4
6 (Biotin)	8481.0 ± 762.6	10671.0 ± 786.5	10281.7 ± 1896.5
α-L-Ara*f*	GBA2 [a]	rhGBA1 [b]	GBA3 [c]
12 (epoxide)	> 50000	> 50000	> 50000
13 (aziridine)	> 50000	> 50000	> 50000
14 (aziridine Cy5)	1850 (30 min) N.D. (3 h)	> 50000 (30 min) 1340 (3 h)	> 50000 (3 h)
β-L-Ara*f*	GBA2 [a]	rhGBA1 [b]	GBA3 [c]
15 (epoxide)	> 20000	> 20000	> 20000
16 (epoxide Cy5)	> 20000	> 20000	> 20000
17 (epoxide BODIPY green)	> 20000	> 20000	> 20000
18 (aziridine)	> 20000	> 20000	> 20000
19 (aziridine Cy5)	> 20000	> 20000	> 20000
20 (aziridine BODIPY green)	20000	> 20000	> 20000

N.D. = not determined, enzyme: [a] GBA2 = GBA1/GBA2 KO and GBA2 OE HEK293T cell lysate, [b] rhGBA1 = isolated Imiglucerase (Cerezyme®), [c] GBA3 = GBA1/GBA2 KO and GBA3 OE HEK293T cell lysate. Incubation time of compounds and enzymes is 30 min, assays was also conducted for 3 h incubation of compound **14** and marked in the table. Error ranges = ± SD, n = 3 replicates for β-D-Ara*f* aziridine compounds, n = 1 replicates for α-L-Ara*f* and β-L-Ara*f* compounds.

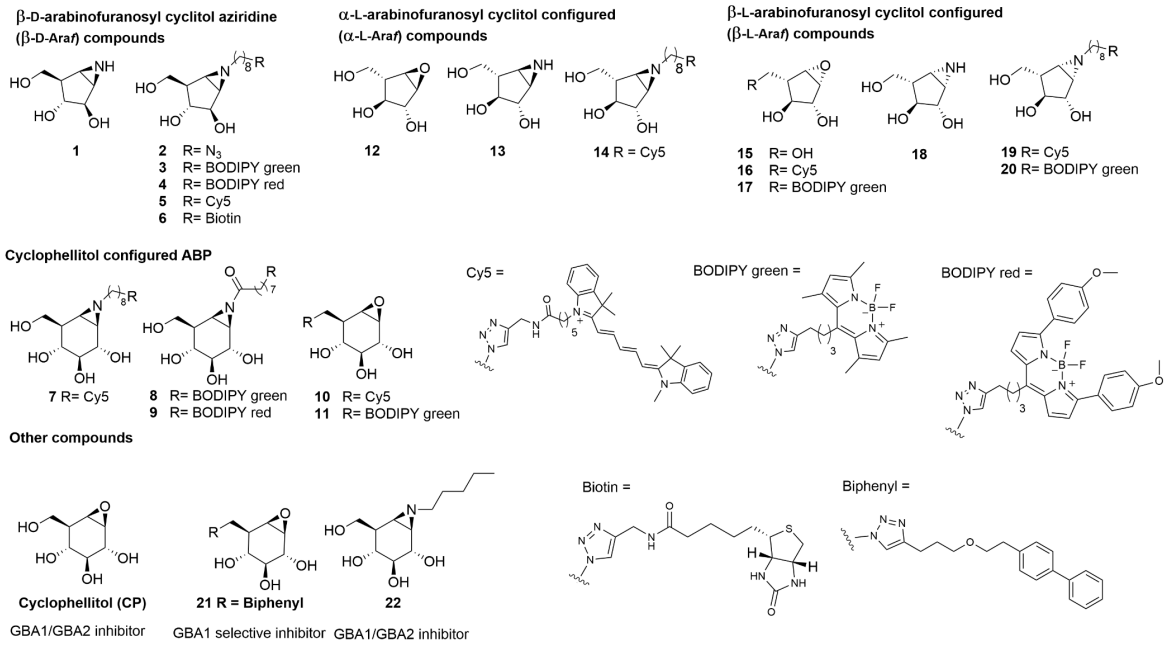

Figure S1. Compound library used in this chapter.

Apparent IC_{50} curves of β-D-Ara*f* compounds

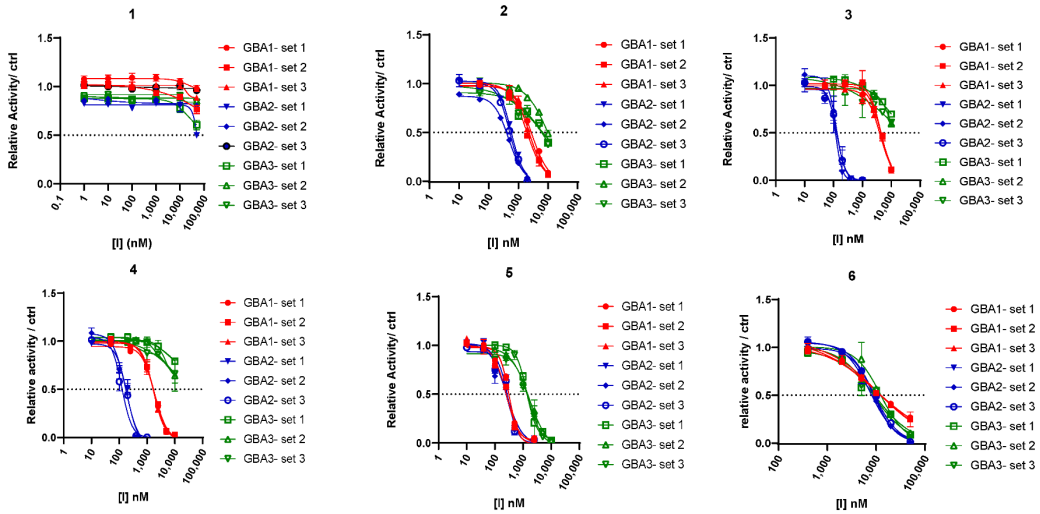

Apparent IC_{50} curves of α-L-Ara*f* compounds

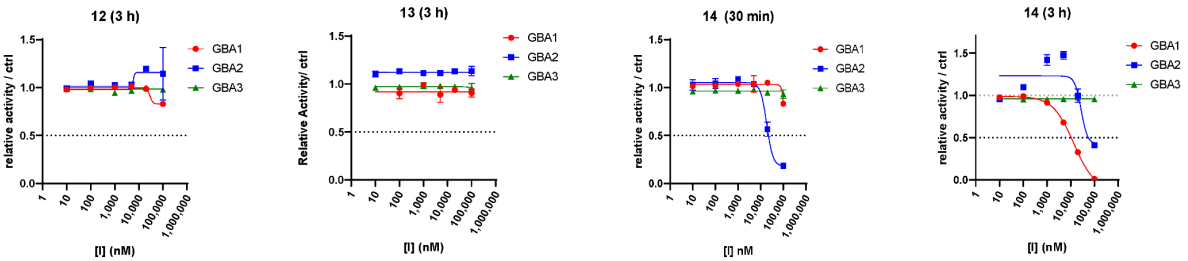

Apparent IC_{50} curves of β-L-Ara*f* compoumds

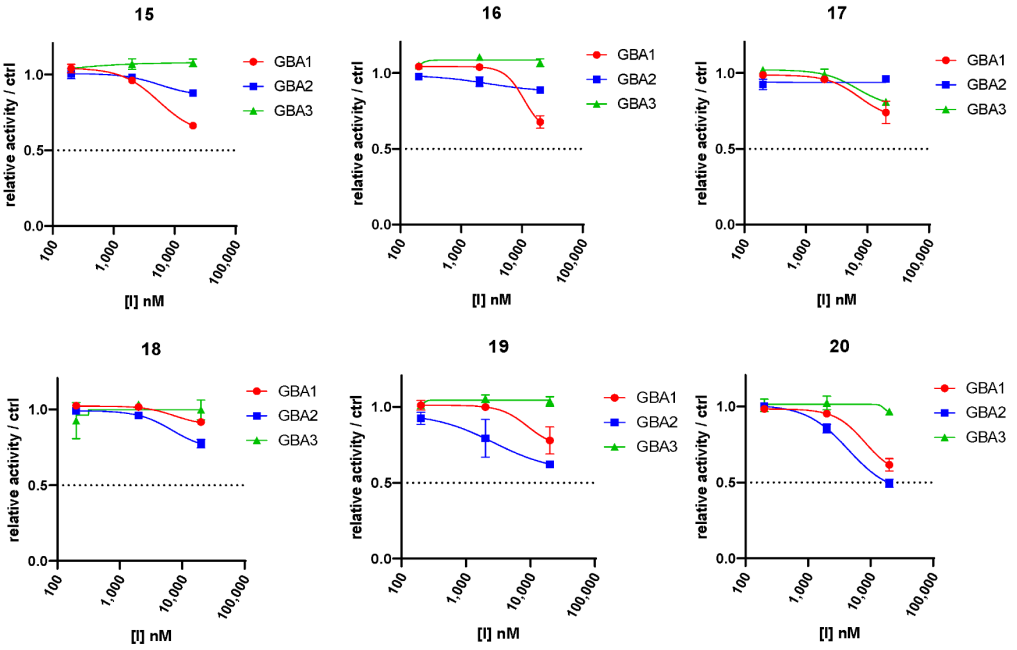

Figure S2. Apparent IC_{50} curves of arabinofuranosyl configured compounds (**1**-**6**, **12**-**20**) based on 4MU fluorogenic substrate assays using 4MU-β-D-Glc. The enzymes used were recombinant GBA1 (Imiglucerase), lysates of GBA1/GBA2 KO cells with overexpression of either GBA2 or GBA3. Incubation time for enzyme with the inhibitors is 30 min (if not otherwise stated) or 3 h (marked as '3 h' in figures) at the appropriate pH.

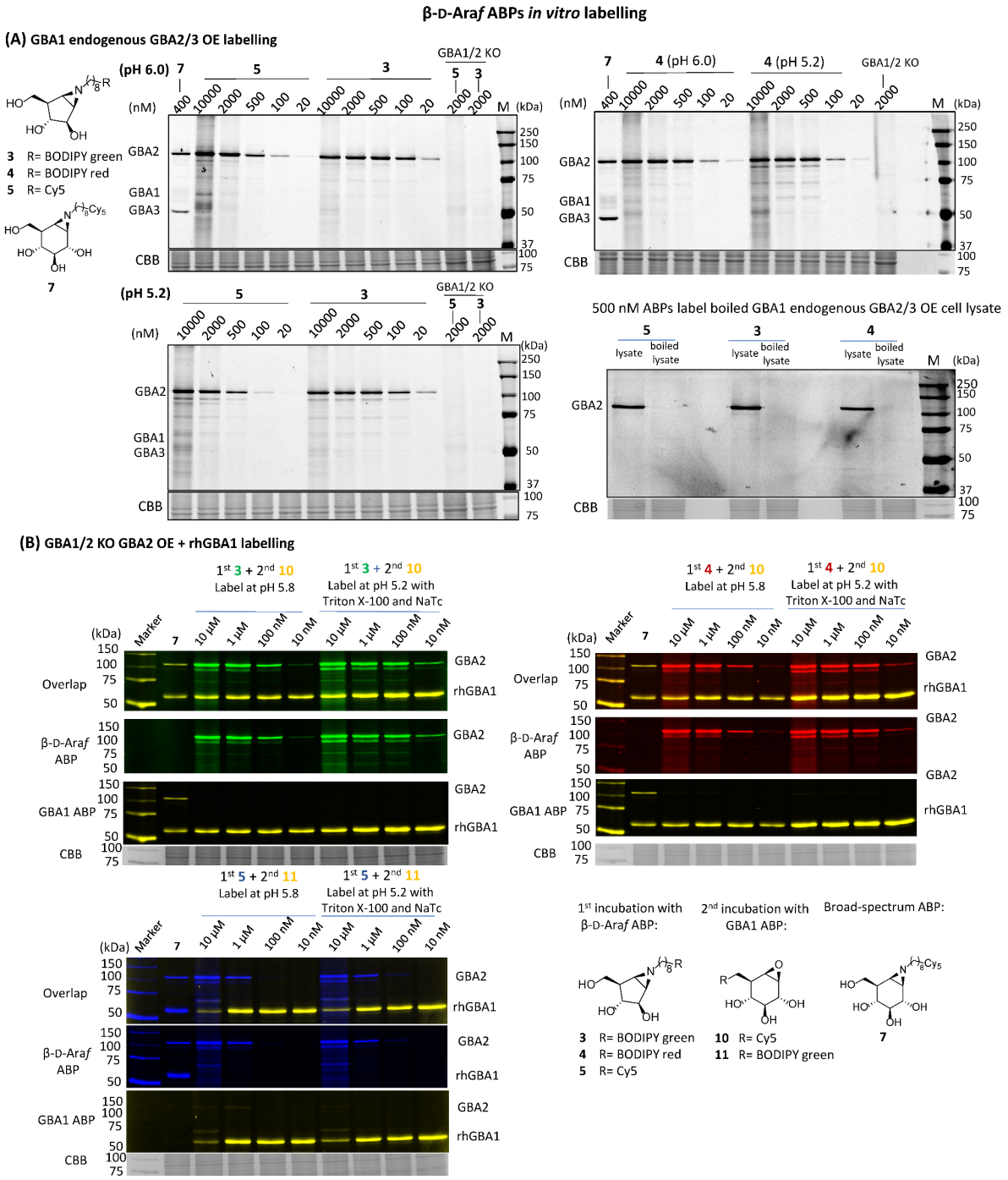

Figure S3-1. *In vitro* reactivity of β-D-Ara*f* aziridine ABPs **3**-**5** towards β-glucosidases. (A) β-D-Ara*f* ABPs incubated with HEK293T GBA1 endogenous and GBA2/GBA3 OE cell lysate *in vitro* for 30 min at 37 °C. To test the activity of ABP **3**-**5** towards boiled lysates (boiled for 5 min at 98 °C). The boiled lysates were incubated with ABPs **3**-**5** for 30 min at 37 °C. Result was read out by SDS-PAGE and fluorescence scanning. (B) β-D-Ara*f* ABPs **3**-**5** labelled mixture of HEK293T GBA1/GBA2 KO GBA2 OE cell lysates and recombinant human GBA1 (rhGBA1) at optimal condtions of GBA2 (left) or rhGBA1 (right). Lysate mixtures were first incubated with β-D-Ara*f* ABPs **3**-**5** for 30 min at 37 °C, followed by labbeling of rhGBA1 by ABP **10** at 500 nM (for **3** and **4**) or ABP **11** at 500 nM (for **5**). Lane marked as '**7**', only ABP **7** was added to show the presence of GBA2 and rhGBA1. To label rhGBA1 at its optimal condition, McIlvaine buffer (pH 5.2) with 0.1% (v/v) Triton X-100 and 0.2% (w/v) sodium taurocholate (NaTc) was used.

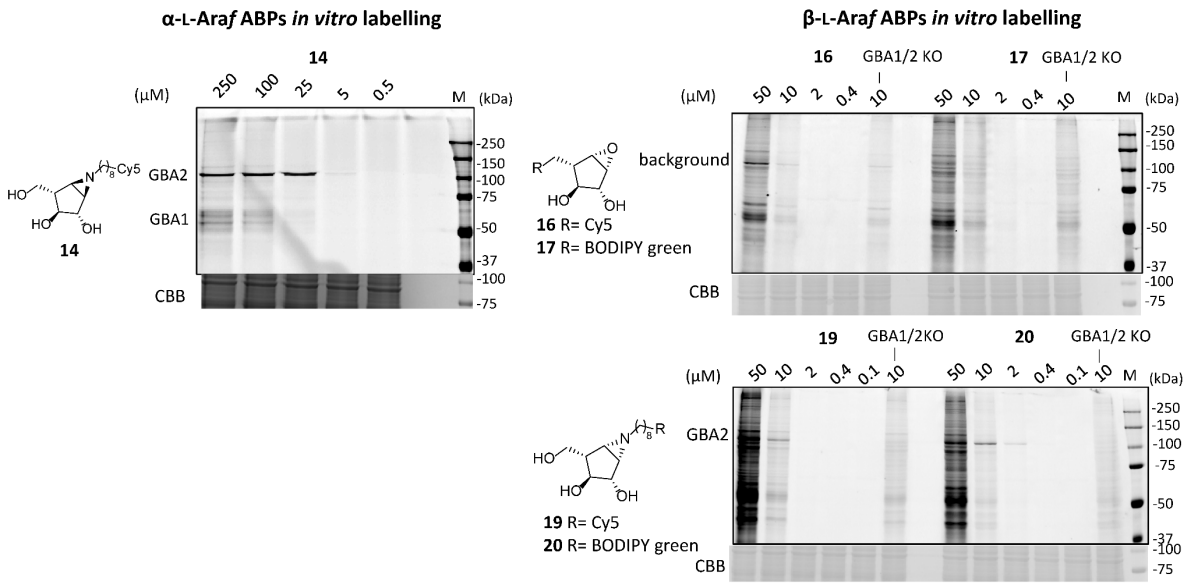

Figure S3-2. Reactivity of α-L-Ara*f* and β-L-Ara*f* ABPs towards β-glucosidases. HEK293T GBA1 endogenous and GBA2/GBA3 OE cell lysates were used and incubated with these ABPs *in vitro* for 30 min at 37 °C, followed by SDS-PAGE and fluorescent scanning of the gels. Coomassie brilliant blue staining (CBB) was performed as a loading control.

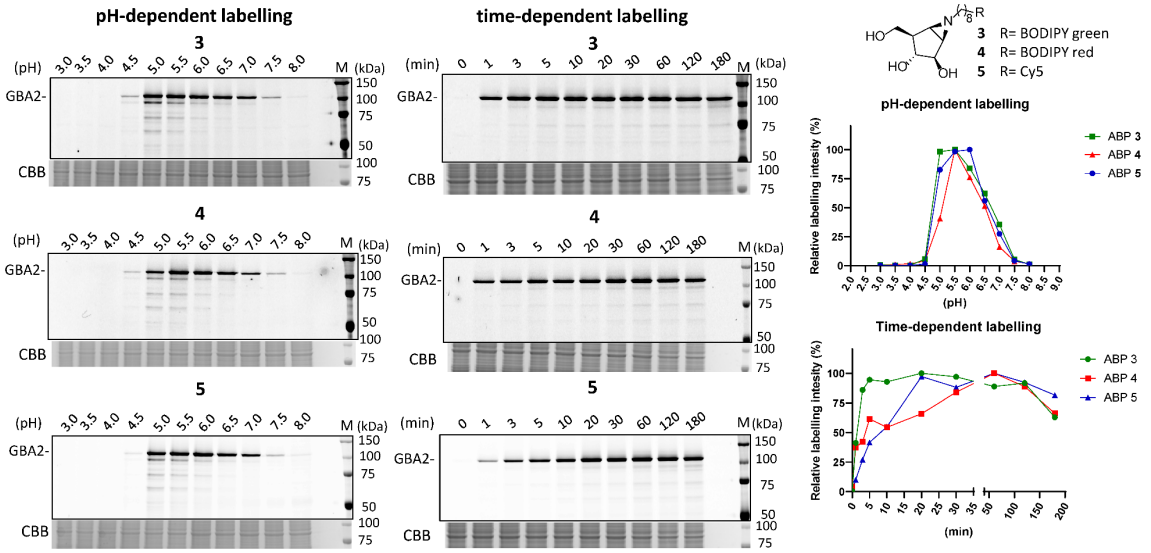

Figure S4. *In vitro* pH- or time-dependent reactivity of β-D-Ara*f* ABPs **3**-**5** (500 nM) towards β-glucosidases. HEK293T GBA1 endogenous and GBA2/GBA3 OE cell lysates were used and incubated with ABP **3**-**5** at the indicated conditions. Fluorescence intensity of ABPs **3**-**5** was quantified and the result was presented as the curve on the right.

The GBA2 interaction efficiency of β-D-Ara*f* aziridine ABPs **3**-**5** and cyclophellitol-aziridine ABP **7** was compared by simultaneous incubation with GBA2 for competition. The mixture of β-D-Ara*f* aziridine ABP (**3**-**5**) against cyclophellitol-aziridine ABP (**7** or **8**) in varying ratios was set up for assays. For each ratio, the amount of total molecules is same (final 500 nM concentration). After incubation, result was read out by SDS-PAGE and fluorescence scanning. As shown in Figure S5, ABP **3** and **4** have equal GBA2 labelling efficiency with ABP **7** at 90:10 ratio (nM of β-D-Ara*f* aziridine ABP : cyclophellitol-aziridine ABP) and ABP **5** only able to label GBA2 at 100:1 ratio when competing with ABP **8**.

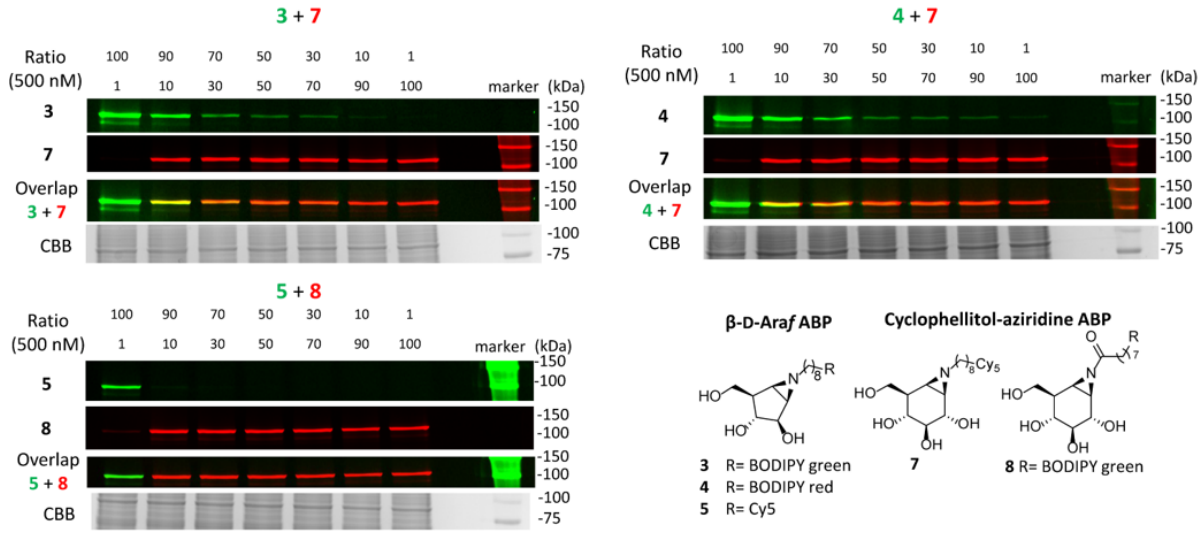

Figure S5. Comparison of the interaction efficiency between β-D-Ara*f* aziridine ABPs (**3**-**5**) and cyclophellitol-aziridine ABPs (**7** or **8**) towards GBA2 *in vitro.* GBA1/GBA2 KO GBA2 OE HEK293T cell lysates were incubated with a total final amount of 500 nM of β-D-Ara*f* ABP and cyclophellitol aziridine ABP **7** (or **8**) mixture in varying ratio as indicated.

To assess the irreversibility of the GBA2 labelling by β-D-Ara*f* cyclitol aziridines, competitive ABPP experiment was conducted. First, lysates of HEK293T GBA1/GBA2 KO cells with GBA2 OE was preincubated with β-D-Ara*f* compound **2**-**4**. After employing a desalting column to remove unbound probe with three consecutive washing steps, the lysate was next incubated with fluorescent broad-spectrum β-glucosidase ABP **7**, an ABP irreversibly binds β-glucosidases, for variable time. No further labelling with **7** was observed compared to the control set (first lane of each set), indicating that the GBA2 molecule had formed a covalent and irreversible bond with β-D-Ara*f* compound **2**-**4**, preventing binding of ABP **7** to GBA2 anymore (Figure S6A). In complementary experiments in which GBA2 lysates were incubated with β-D-Ara*f* compounds **2**-**5** followed by washing to remove any unbound probe, no recovery of GBA2 activity was observed even after 96 h (Figure S6C).

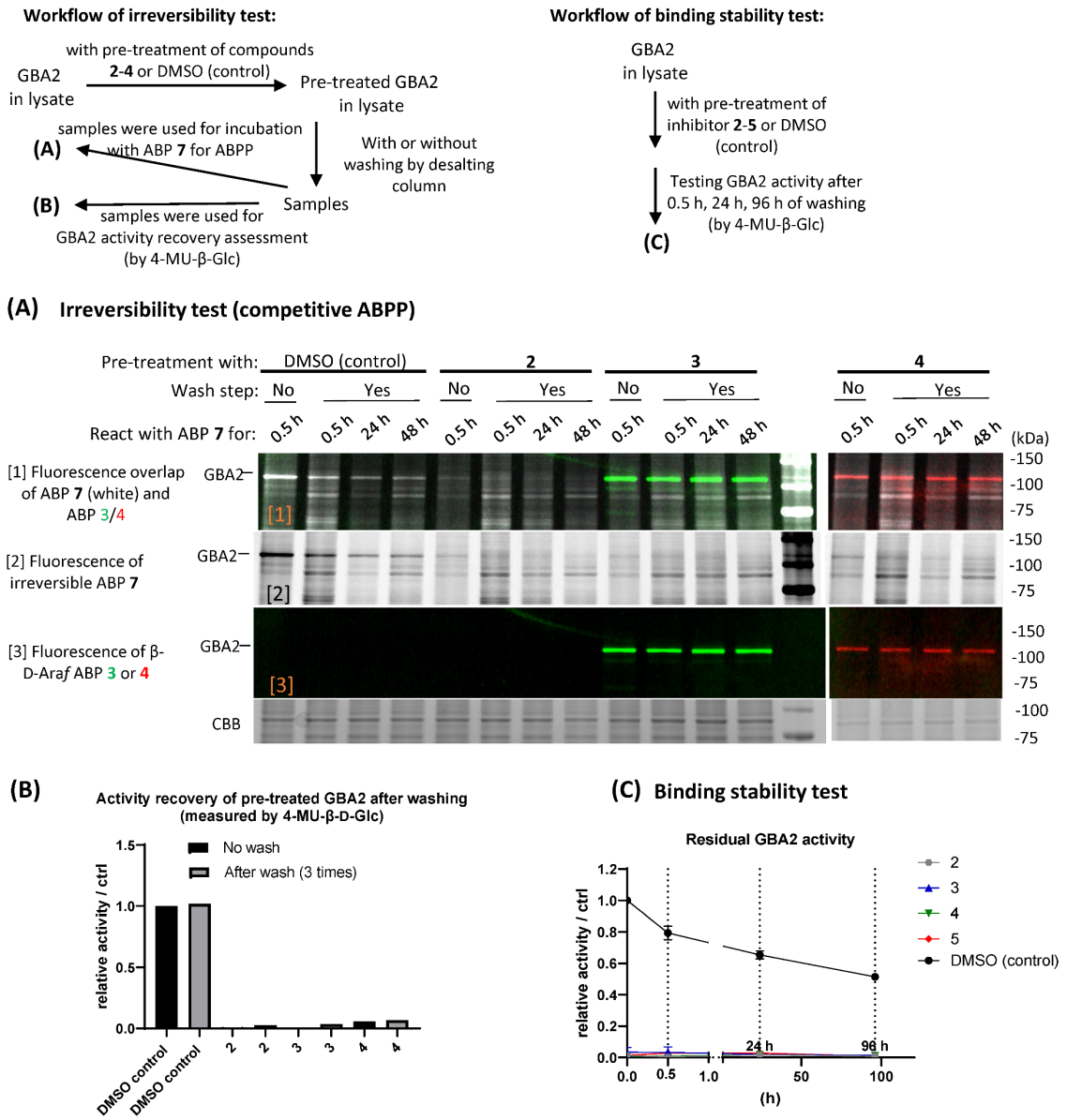

Figure S6. (A) Irreversibility of β-D-Ara*f* aziridine compounds revealed by a competition ABPP assay. Lysates of GBA1/GBA2 KO cells with GBA2 overexpression were first pre-treated with the β-D-Ara*f* compounds **2**-**4** or an equivalent volume without compound (0.5% DMSO final concentration in this step as control) for 30 min at 37°C, followed by three times of consecutive washing with a desalting column and incubation with 1 µM irreversible ABP **7** for 30 min (for competition analysis) after the washing step, the final concentration of DMSO in all samples after addition of ABP **7** was maintained at 1%. Lanes: 'No wash, 0.5 h' = GBA2 pre-treated with compounds **2**-**4** or DMSO, without undergoing the washing steps, followed by incubating with ABP **7** for 0.5 h at 37 °C. The samples that underwent the washing step (lanes marked with 'wash step, yes'), were incubated either with ABP **7** for 24 h or 48 h at 4 °C (for enzyme stability reasons), or with ABP **7** for 0.5 h at 37 °C. Afterwards, samples were subjected to ABPP. (B) A subset of above samples pre-treated with compounds **2**-**4** or DMSO, were washed three times with a desalting column, subsequently, samples were measured for GBA2 activity by the 4-MU-β-D-Glc fluorogenic substrate assay, to assess whether GBA2, which had reacted with compounds **2**-**4**, could recover activity after the washing step. (C) Binding stability of compounds **2**-**5** towards GBA2 revealed by the 4-MU-β-D-Glc fluorogenic substrate assay. Lysates of GBA1/GBA2 KO cells with GBA2 overexpression were pre-treated with compounds **2**-**5** or an equivalent volume of DMSO (as control) and washed once by a desalting column, then the lysates were stored at 4°C until the time point for activity measurement was reached. 0 h = measured activity of lysates prior to washing by desalting column. '0.5 h, 24 h, or 96 h' = measured activity of lysates at a certain time point after washing steps.

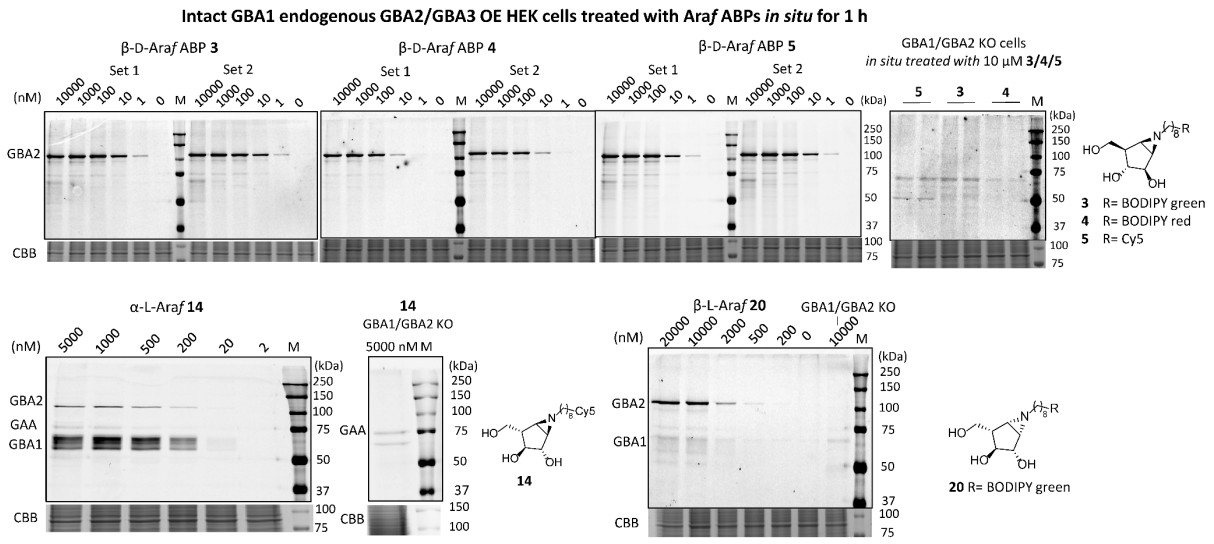

Figure S7. Intact HEK293T cells, either with endogenous GBA1 and GBA2/GAB3 OE, or with GBA1/GBA2 KO, were incubated with arabinofuranosyl cyclitol configured ABPs (**3**-**5**, **14**, **20**) for 1 h *in situ*, then cells were lysed and subjected to ABPP. GAA = Lysosomal α-glucosidase (EC 3.2.1.20, CAZy GH31).

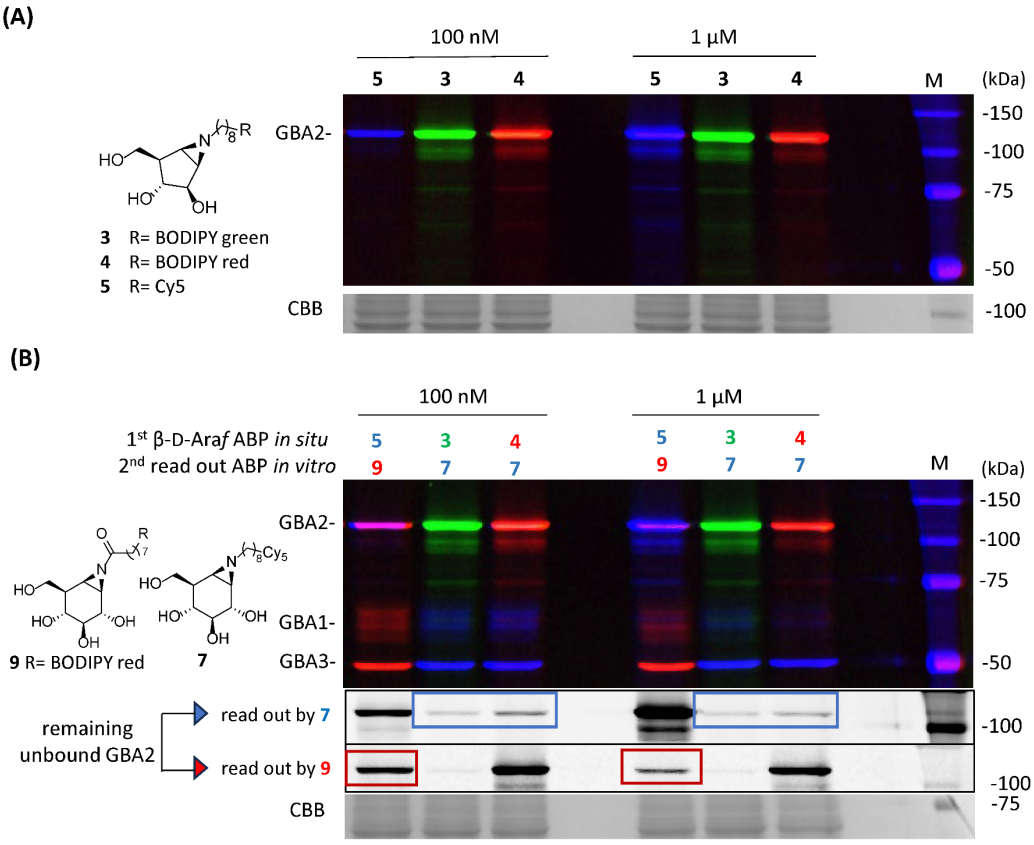

Figure S8. β-D-Ara*f* aziridine ABPs incubated with intact HEK293T cells (endogenous GBA1 and GBA2/GBA3 OE) for 24 h *in situ*. Intact HEK293T cells were treated with β-D-Ara*f* ABPs (**3**-**5**) for 24 h at 37 °C under 7% CO_2, then cells were collected and lysed, followed by ABPP. (A) ABPP of intact cells labelled by β-D-Ara*f* ABPs (**3**-**5**) *in situ*. (B) Intact cells labelled by β-D-Ara*f* ABPs (**3**-**5**) *in situ* were lysed and followed by *in vitro* incubation with 500 nM broad-spectrum β-glucosidase ABP **7** (for **3** and **4**) or **11** (for **5**), to reveal residual active β-glucosidases not bound by ABP **3**-**5**.

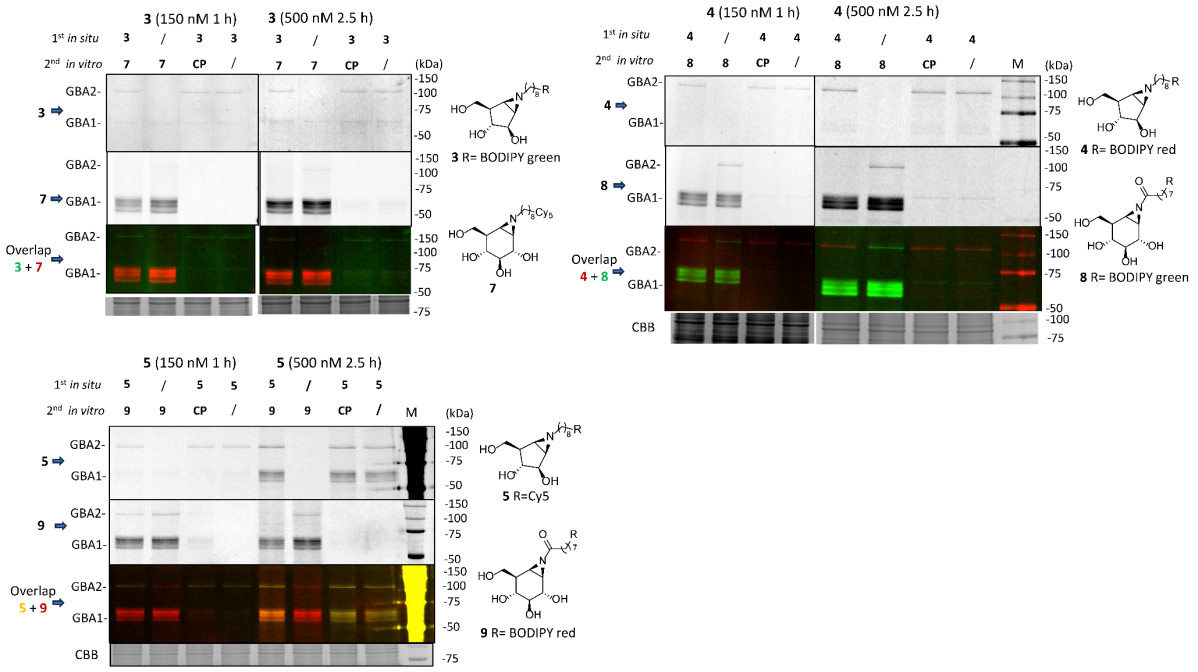

Figure S9. Intact wild-type HEK293T cells treated with β-D-Ara*f* aziridine ABPs (**3**-**5**) *in situ*. β-D-Ara*f* ABPs were firstly incubated with intact wild-type HEK293T *in situ* for the indicated incubation time, then cells were harvested, followed by adding lysis buffer (potassium phosphate buffer) containing ABP (**7**, **8**, or **9**, 1 μM final concentration with a 1% DMSO final concentration), or cyclophellitol (**CP**, 1 μM final concentration with a 1% DMSO final concentration), or the blank ('/') 1% DMSO (final concentration) for ABPP analysis. Then harvested cells were lysed in lysis buffer and incubated for 30 min on ice and 30 min at 37°C *in vitro* for ABPP.

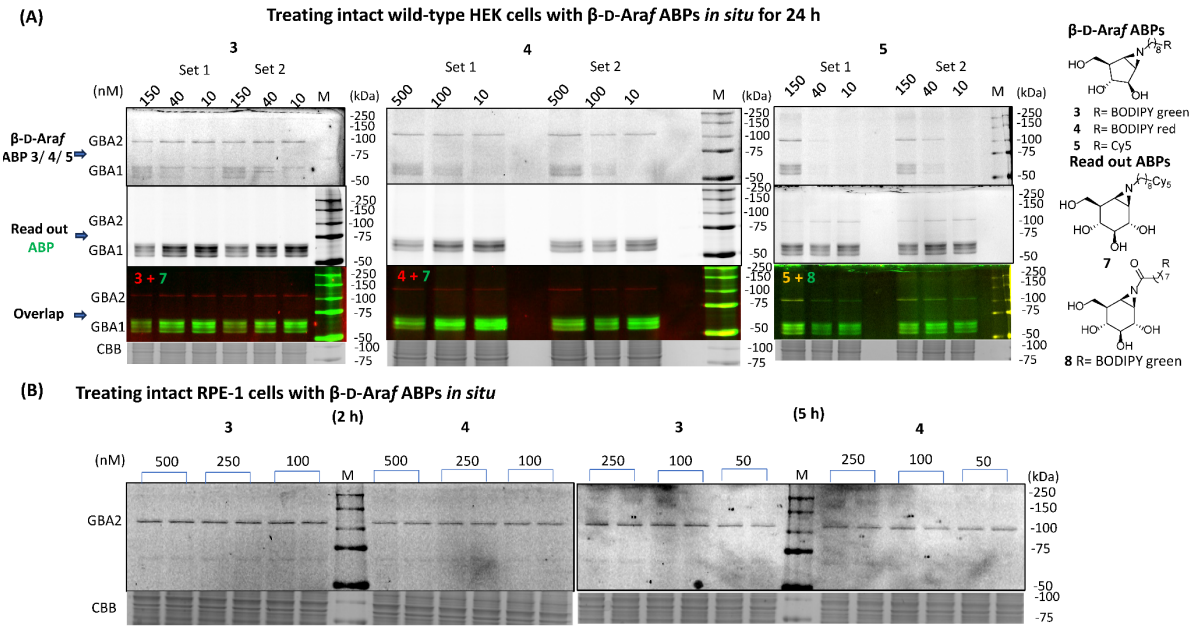

Figure S10. (A) Intact HEK293T wild-type cells treated with β-D-Ara*f* aziridine ABPs **3**-**5** *in situ* for 24 h. Intact wild-type HEK293T cells were incubated with described concentration of β-D-Ara*f* ABP, after 24 h, cells were collected and lysed, residual GBA2 and GBA1 activity were read out by incubation with 500 nM ABP **7** (for **3** and **4**) or ABP **8** (for **5**). (B) Wild-type human retinal pigment epithelial-1 (RPE-1) cells were treated with β-D-Ara*f* aziridine ABPs **3**-**5** for either 2 h or 5 h *in situ*. Then cells were collected, lysed, and subjected to ABPP.

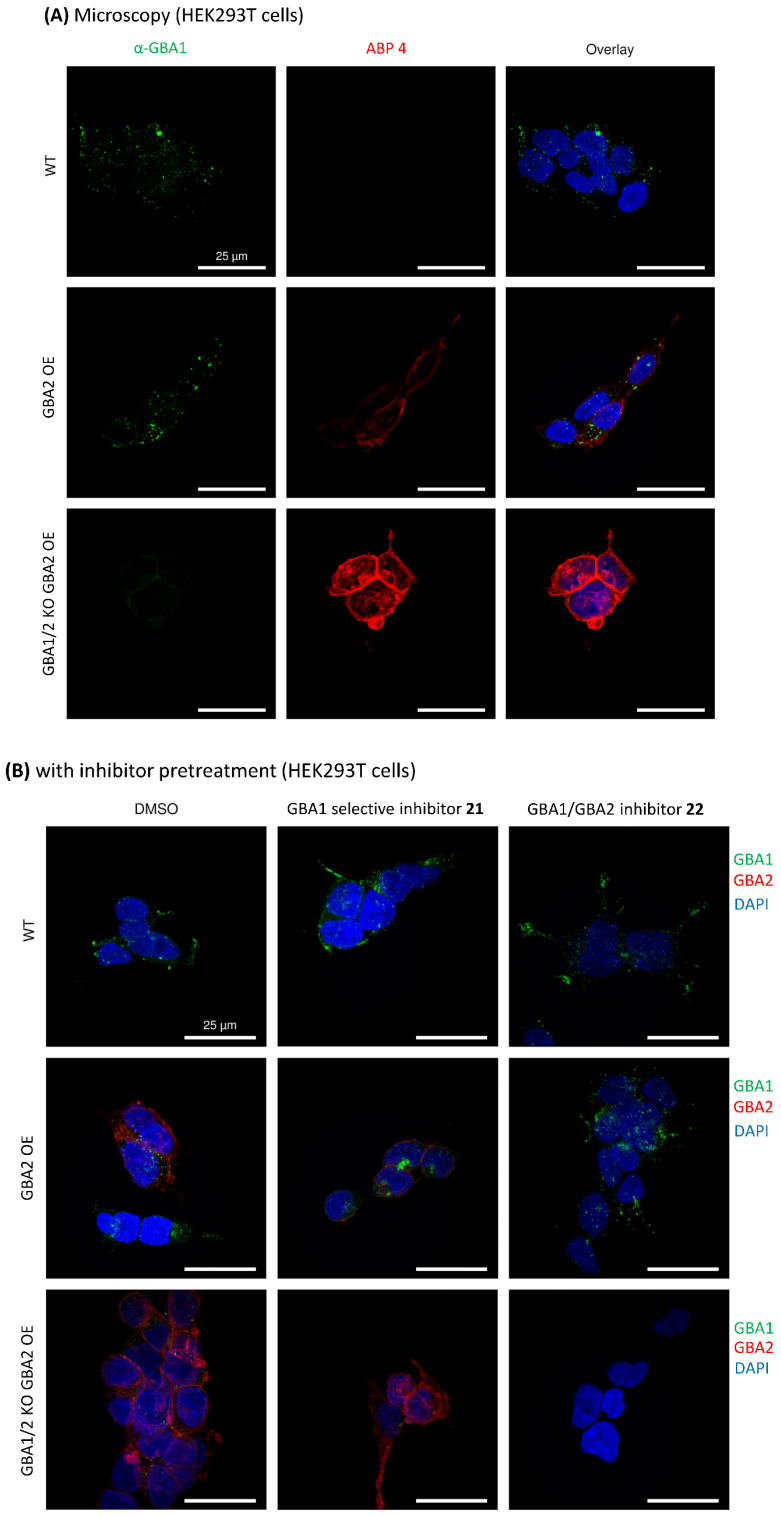

Figure S11. Confocal fluorescence microscopy of GBA1 and GBA2. Applied for incubation were β-D-Ara*f* ABP **4** and anti-GBA1 (α-GBA1) antibody. Used were different HEK293T cells: HEK293T wild-type (WT), GBA2 overexpression (OE), and GBA1/GBA2 knock out (KO) with GBA2 overexpression (OE). Cells were treated with 50 nM β-D-Ara*f* aziridine ABP **4** (Red) for 2 h. After fixation all cells were stained for GBA1 using an anti-GBA1-antibody with Alexa Fluor® 647 conjugation (green) and nuclei were stained with 10 µg/ml DAPI (Blue). (A) without inhibitor pretreatment. α-GBA1 = immunofluorescent stain of α-GBA1 antibody, GBA2 = fluorescent labelling of ABP **4**, DAPI = nuclei stained by DAPI. (B) microscopy with inhibitor pretreatment. DMSO = same concentration of DMSO (as sets of **21** and **22**) without inhibitor was added (pre-treatment). 100 nM **21** and 500 nM **22** were used for the inhibitor pretreatments.

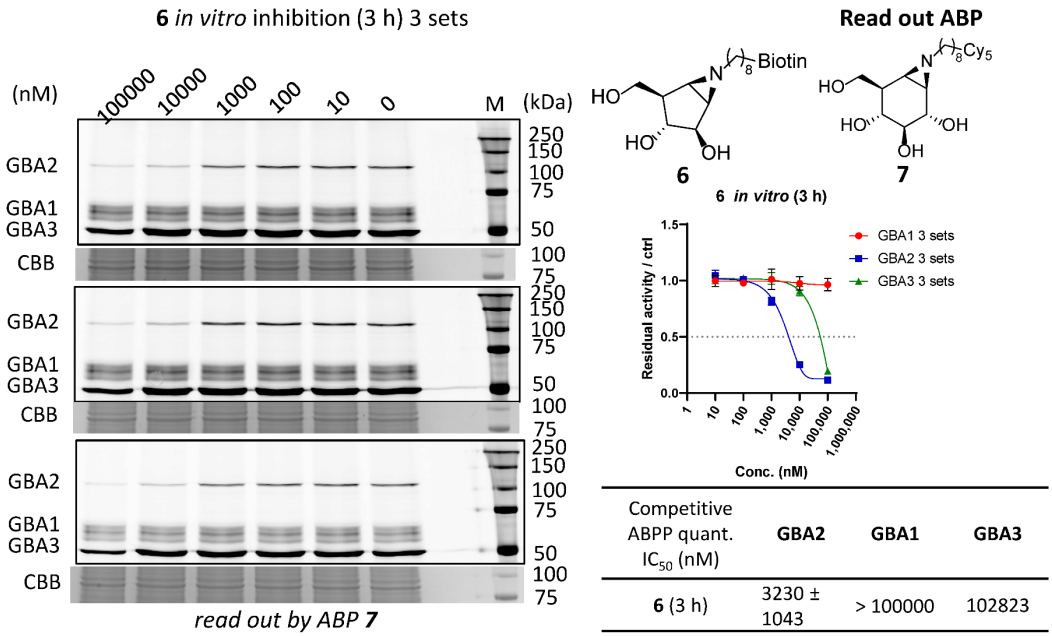

Competitive ABPP quant. IC_{50} (nM)	GBA2	GBA1	GBA3
6 (3 h)	3230 ± 1043	> 100000	102823

Figure S12. Assessment of the affinity and selectivity of a biotin-tagged compound **6** via *in vitro* competitive ABPP assay. Lysates of HEK293T GBA1 endogenous and GBA2/GBA3 OE cell were pre-treated with **6** for a 3 h incubation at 37 °C, then the residual active β-glucosidases were read out by 500 nM ABP **7** by competitive ABPP quantified IC_{50} was determined by the fluorescence intensity of ABP **7**.

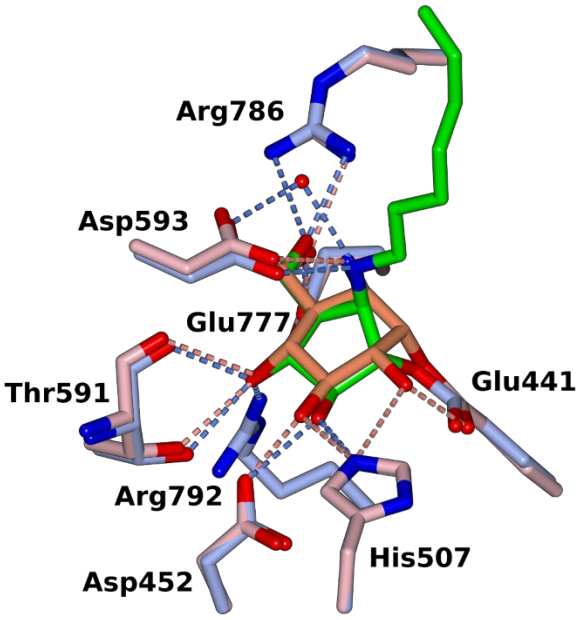

Figure S13. Overlay of structures of *Tx*GH116 complexes with cyclophellitol aziridine (8R06.pdb) and compound **2** (8R1M.pdb). C atoms are shown in orange for cyclophellitol aziridine and light pink for interacting side chains (with hydrogen bonds as coral dashed lines), and in green for **2** and ice blue for interacting side chains (with hydrogen bonds as blue dashed lines).

Table S2. Data collection and refinement statistics for the complex of *Tx*GH116 and β-D-Ara*f* **2**.

	***Tx*GH116-2**
Data collection	
Space group	P 21 21 21
Cell dimensions	
a, *b*, *c* (Å)	55.0, 165.1, 178.9
α, β, γ (°)	90.0, 90.0, 90.0
Resolution (Å)	56.09 – 1.90 (1.93 - 1.90)*
Total no. reflections	1381158
No. unique reflections	129333 (6302)
R_{sym} or R_{merge}	0.249 (2.052)
R_{pim}	0.079 (0.643)
$CC_{1/2}$	0.996 (0.554)
$I / \sigma I$	7.1 (1.3)
Completeness (%)	100.0 (100.0)
Redundancy	10.7 (10.9)
Refinement	
No. reflections working set	122902
No. reflections test set	6306
R_{work} / R_{free}	0.18/0.23
No. atoms	
Protein	12592
Ligand/ion	53
Water	880
B-factors	
Protein	24.9
Ligand/ion	31.9
Water	29.9
R.m.s deviations	
Bond lengths (Å)	0.006
Bond angles (°)	1.513
Ramachandran plot residues	
In most favorable regions (%)	95.1
In allowed regions (%)	4.4
PDB code	8R1M

* Figures for highest resolution shell given in parentheses

Compound synthesis

Compounds used in this work were synthesized and obtained at the Bio-organic Synthesis Department, Leiden Institute of Chemistry at Leiden University, according to published methods:

β-D-arabinofuranosyl cyclitol-aziridines : **1**,[1] **2**-**6**.[2]

α-L-arabinofuranosyl cyclitol-configured compounds: **12-14**.[3]

β-L-arabinofuranosyl cyclitol-configured compounds: **15**[4] and **16-20**[5].

Cyclophellitol-configured compounds: **7**[6], **8**[7], **9**[8], **10**[9] and **11**[10].

Other compounds: **21**[9], **22**[11].

Supplementary references

1. O. Lopez Lopez, J. G. Fernandez-Bolanos, V. H. Lillelund and M. Bols, Aziridines as a structural motif to conformational restriction of azasugars, *Org. Biomol. Chem.*, 2003, **1**, 478-482.
2. S. P. Schröder, Cyclophellitol analogues for profiling of exo- and endo-glycosidases, Thesis, Leiden University, 2018, https://hdl.handle.net/1887/62362.
3. N. G. S. McGregor, M. Artola, A. Nin-Hill, D. Linzel, M. Haon, J. Reijngoud, A. Ram, M. N. Rosso, G. A. van der Marel, J. D. C. Codée, G. P. van Wezel, J. G. Berrin, C. Rovira, H. S. Overkleeft and G. J. Davies, Rational design of mechanism-based inhibitors and activity-based probes for the identification of retaining alpha-l-arabinofuranosidases, *J. Am. Chem. Soc.*, 2020, **142**, 4648-4662.
4. N. G. S. McGregor, J. Coines, V. Borlandelli, S. Amaki, M. Artola, A. Nin-Hill, D. Linzel, C. Yamada, T. Arakawa, A. Ishiwata, Y. Ito, G. A. van der Marel, J. D. C. Codée, S. Fushinobu, H. S. Overkleeft, C. Rovira and G. J. Davies, Cysteine nucleophiles in glycosidase catalysis: application of a covalent beta-l-arabinofuranosidase inhibitor, *Angew. Chem. Int. Ed.*, 2021, **60**, 5754-5758.
5. V. Borlandelli, W. Offen, O. Moroz, A. Nin-Hill, N. McGregor, L. Binkhorst, A. Ishiwata, Z. Armstrong, M. Artola, C. Rovira, G. J. Davies and H. S. Overkleeft, beta-l-Arabinofurano-cyclitol aziridines are covalent broad-spectrum inhibitors and activity-based probes for retaining beta-l-arabinofuranosidases, *ACS Chem. Biol.*, 2023, **18**, 2564-2573.
6. S. P. Schröder, J. W. van de Sande, W. W. Kallemeijn, C. L. Kuo, M. Artola, E. J. van Rooden, J. Jiang, T. J. M. Beenakker, B. I. Florea, W. A. Offen, G. J. Davies, A. J. Minnaard, J. M. Aerts, J. D. C. Codée, G. A. van der Marel and H. S. Overkleeft, Towards broad spectrum activity-based glycosidase probes: synthesis and evaluation of deoxygenated cyclophellitol aziridines, *Chem. Commun.*, 2017, **53**, 12528-12531.
7. W. W. Kallemeijn, K. Y. Li, M. D. Witte, A. R. Marques, J. Aten, S. Scheij, J. Jiang, L. I. Willems, T. M. Voorn-Brouwer, C. P. van Roomen, R. Ottenhoff, R. G. Boot, H. van den Elst, M. T. Walvoort, B. I. Florea, J. D. Codée, G. A. van der Marel, J. M. Aerts and H. S. Overkleeft, Novel activity-based probes for broad-spectrum profiling of retaining beta-exoglucosidases in situ and in vivo, *Angew. Chem. Int. Ed.*, 2012, **51**, 12529-12533.
8. K.-Y. Li, J. Jiang, M. D. Witte, W. W. Kallemeijn, H. van den Elst, C.-S. Wong, S. D. Chander, S. Hoogendoorn, T. J. M. Beenakker, J. D. C. Codée, J. M. Aerts, G. A. van der Marel and H. S. Overkleeft, Synthesis of cyclophellitol, cyclophellitol aziridine, and their tagged derivatives, *Eur. J. Org. Chem.*, 2014, **2014**, 6030-6043.
9. M. Artola, C. L. Kuo, L. T. Lelieveld, R. J. Rowland, G. A. van der Marel, J. D. C. Codée, R. G. Boot, G. J. Davies, J. M. Aerts and H. S. Overkleeft, Functionalized cyclophellitols are selective glucocerebrosidase inhibitors and induce a bona fide neuropathic Gaucher model in zebrafish, *J. Am. Chem. Soc.*, 2019, **141**, 4214-4218.
10. M. D. Witte, W. W. Kallemeijn, J. Aten, K. Y. Li, A. Strijland, W. E. Donker-Koopman, A. M. van den Nieuwendijk, B. Bleijlevens, G. Kramer, B. I. Florea, B. Hooibrink, C. E. Hollak, R. Ottenhoff, R. G. Boot, G. A. van der Marel, H. S. Overkleeft and J. M. Aerts, Ultrasensitive in situ visualization of active glucocerebrosidase molecules, *Nat. Chem. Biol.*, 2010, **6**, 907-913.
11. K. Y. Li, J. Jiang, M. D. Witte, W. W. Kallemeijn, W. E. Donker-Koopman, R. G. Boot, J. M. Aerts, J. D. Codée, G. A. van der Marel and H. S. Overkleeft, Exploring functional cyclophellitol analogues as human retaining beta-glucosidase inhibitors, *Org. Biomol. Chem.*, 2014, **12**, 7786-7791.